Geosci. Model Dev., 5, 919–940, 2012
www.geosci-model-dev.net/5/919/2012/
doi:10.5194/gmd-5-919-2012

Geoscientific Model Development

MAESPA: a model to study interactions between water limitation, environmental drivers and vegetation function at tree and stand levels, with an example application to $[CO_2]$ × drought interactions

R. A. Duursma[1] **and B. E. Medlyn**[2]

[1]Hawkesbury Institute for the Environment, University of Western Sydney, Locked Bag 1797, Penrith, NSW 2751, Australia
[2]Department of Biological Sciences, Macquarie University, North Ryde, NSW 2109, Australia

Correspondence to: R. A. Duursma (remkoduursma@gmail.com)

Received: 8 December 2011 – Published in Geosci. Model Dev. Discuss.: 17 February 2012
Revised: 5 June 2012 – Accepted: 8 June 2012 – Published: 5 July 2012

Abstract. Process-based models (PBMs) of vegetation function can be used to interpret and integrate experimental results. Water limitation to plant carbon uptake is a highly uncertain process in the context of environmental change, and many experiments have been carried out that study drought limitations to vegetation function at spatial scales from seedlings to entire canopies. What is lacking in the synthesis of these experiments is a quantitative tool incorporating a detailed mechanistic representation of the water balance that can be used to integrate and analyse experimental results at scales of both the whole-plant and the forest canopy. To fill this gap, we developed an individual tree-based model (MAESPA), largely based on combining the well-known MAESTRA and SPA ecosystem models. The model includes a hydraulically-based model of stomatal conductance, root water uptake routines, drainage, infiltration, runoff and canopy interception, as well as detailed radiation interception and leaf physiology routines from the MAESTRA model. The model can be applied both to single plants of arbitrary size and shape, as well as stands of trees. The utility of this model is demonstrated by studying the interaction between elevated $[CO_2]$ (eC_a) and drought. Based on theory, this interaction is generally expected to be positive, so that plants growing in eC_a should be less susceptible to drought. Experimental results, however, are varied. We apply the model to a previously published experiment on droughted cherry, and show that changes in plant parameters due to long-term growth at eC_a (acclimation) may strongly affect the outcome of $C_a \times$ drought experiments. We discuss potential applications of MAESPA and some of the key uncertainties in process representation.

1 Introduction

The response of plant carbon uptake and water use to environmental change is complex because there are many interactions and feedbacks that modify the response to single environmental drivers. This complexity is highlighted by the remarkable diversity of experimental outcomes, for example in the response of plant water use and carbon uptake to elevated atmospheric $[CO_2]$ (Ainsworth and Long, 2005; Ainsworth and Rogers, 2007; Norby et al., 1999), warming (Rustad et al., 2001), and soil water deficit (Manzoni et al., 2011; Wu et al., 2011). Soil water availability frequently limits plant productivity, but because of interactions with plant properties, and with other environmental drivers, it remains difficult to predict the effect on vegetation water use and carbon uptake (Hanson et al., 2004). Because soil drought is already becoming more frequent as a result of climate change (Huntington, 2006), it is crucial that its effect on vegetation function is more readily quantifiable.

Process-based models (PBMs) can be used as a research tool to clarify interactions among environmental drivers, plant and canopy structure, leaf physiology and soil water availability and their combined effects on water use and carbon uptake (Luo et al., 2008; Norby and Luo, 2004; Williams et al., 2001b). Because PBMs summarize the state-of-art theory of plant functioning in a coherent quantitative framework, they provide a way forward for testing our understanding of how plants respond to environmental change. In this way, they might be used to improve on empirical meta-analyses of experiments. These meta-analyses have been crucial in determining overall responses of vegetation to manipulation of the environment, but the variability among

experiments remains incompletely understood (Poorter and Navas, 2003). Meta-analyses usually focus on the effect of a single variable on vegetation function, although it has been recognized that interactions, feedbacks and acclimation are important in determining overall experimental outcomes (Norby and Luo, 2004; Norby et al., 1999; Wullschleger et al., 2002).

Typical experiments or long-term observations are conducted at spatial scales from whole plants (potted seedlings, whole-tree chambers) to entire canopies (eddy-covariance sites, free-air CO_2 enrichment; FACE). A useful PBM to analyse and integrate experiments should therefore operate at both whole-plant and canopy scales. Another requirement is that the PBM incorporate detailed water balance routines and hydraulics of the soil-plant pathway.

Currently, no PBM exists that meets both requirements, and is sufficiently detailed to allow a connection with typical measurements of plant physiological function and plant canopy structure. Here, we introduce a new model, MAESPA, based on a combination of the well-known MAESTRA and SPA models.

The MAESTRA model is a tree array model that uses detailed radiative transfer calculations and leaf physiology to calculate radiation absorption, photosynthesis and transpiration of individual trees, growing singly or in a population (Medlyn, 2004; Wang and Jarvis, 1990). The MAESTRA model has been applied in a wide range of contexts from horticulture (e.g. Bauerle and Bowden, 2011) to regional climate change (e.g. Luxmoore et al., 2000), resulting in well over fifty publications (Medlyn, 2004; updated bibliography available at www.bio.mq.edu.au/maestra/bibliog.html). A major limitation of this model, however, has been the lack of a dynamic water balance. Medlyn et al. (2005) added the capacity to input soil moisture and thereby estimate the effect of a given soil moisture stress on photosynthesis and transpiration (e.g. as used by Reynolds et al., 2009), but the model does not calculate the soil moisture dynamically. This lack severely limits model applications in dry conditions because feedbacks to plant performance via soil moisture cannot be simulated. For example, although the model has often been used to estimate effects of elevated atmospheric [CO_2] (C_a) on canopy performance (e.g. Kirschbaum et al., 1994; Medlyn, 1996; Kruijt et al., 1999; Luo et al., 2001), the model cannot be used to investigate elevated [CO_2] impacts in drought conditions because it is not possible to calculate how elevated [CO_2] modifies soil moisture.

The SPA model (Williams et al., 2001a, b) is another well-known process-based model, with a focus on the impacts of water availability on forest canopies. However, this model is also limited in that it assumes a horizontally homogenous canopy and thus does not allow for applications to individual trees. We added to MAESTRA the detailed soil water balance routines from the SPA model (Williams et al., 2001a, b), thus combining the strengths of the two models into a new soil-plant-atmosphere model that accounts for non-homogenous stand structure. In addition, we made a number of improvements to the combined model that allow a detailed physiologically-based analysis of the complete soil-plant-atmosphere pathway. We believe that the new, combined model is a significant advance over either MAESTRA or SPA and will prove a useful tool for researchers in forest ecophysiology. Our goals in this paper are to fully document the new model and to demonstrate its use by applying it to a previously intractable question, namely the interaction between atmospheric [CO_2] (C_a) and drought.

Numerous experiments have been carried out on the interaction of C_a and drought on plant functioning (see reviews by Rogers et al., 1994 and Wullschleger et al., 2002). A simple prediction for this interaction is that the C_a response will be higher under soil drought for two reasons: firstly, lower leaf-level water use under eC_a (Eamus, 1991; Medlyn et al., 2001) leads to higher soil water content, which helps plants avoid soil water deficits; and secondly, lower intercellular CO_2 concentration (C_i) during drought enhances the C_a response because of the non-linear response of photosynthetic rate to C_i (Grossman-Clarke et al., 2001; McMurtrie et al., 2008). While both mechanisms have been confirmed in a number of crop and grassland studies (e.g. Morgan et al., 2004; Rogers et al., 1994), experiments with potted tree seedlings, trees in whole-tree chambers or entire canopies in FACE experiments have yielded highly variable results (Gunderson et al., 2002; Nowak et al., 2004; Warren et al., 2010; Duursma et al., 2011). Two mechanisms are likely responsible for this variability in experimental outcomes: feedbacks from eC_a-induced changes in plant size on water use and soil water balance; and acclimation of leaf physiology to long-term growth at eC_a. We first study the response of plant carbon uptake and water use to a simulated dry-down, which is a useful baseline for comparison with actual experimental outcomes. We then study the effects of acclimation of two leaf physiology parameters on the $C_a \times$ drought interaction. Finally, we apply the MAESPA model to a $C_a \times$ drought experiment where a feedback of increased leaf area in the eC_a treatment confounds the direct effect of C_a, and show how analysis of experimental data within a model-based framework can extend basic empirical results.

2 Methods

2.1 Model description

2.1.1 Overview

In the following, we describe the MAESPA model, which is largely the product of the above-ground components of the MAESTRA model (Wang and Jarvis, 1990; Medlyn et al., 2007) and the water balance components of the SPA model (Williams et al., 2001a, b), with several modifications and additions (see Table 1). The MAESTRA model has its roots in

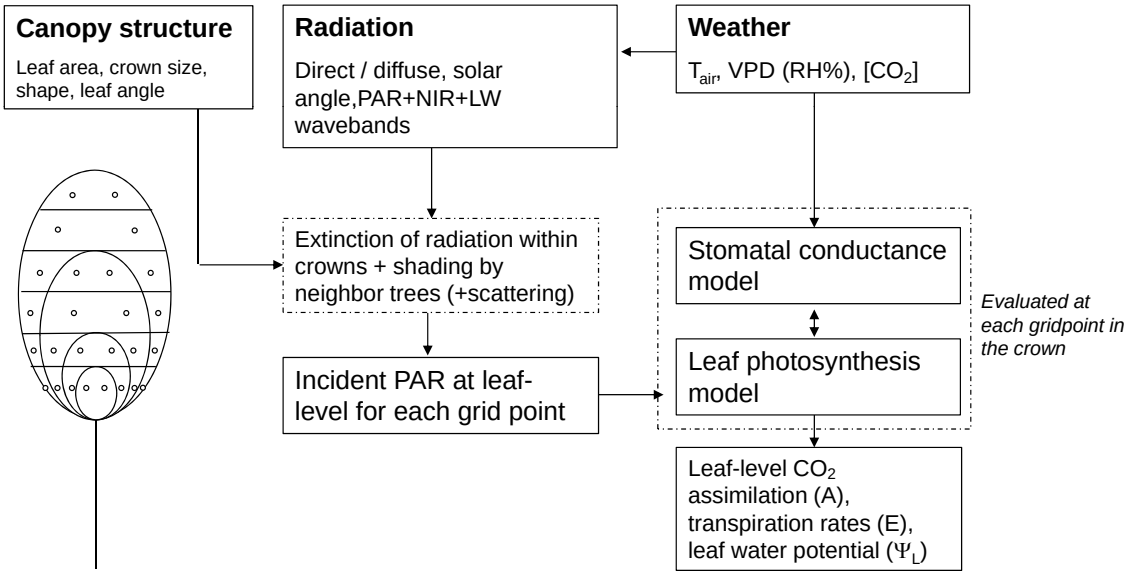

Fig. 1. Flowchart of MAESTRA, the above-ground model of the MAESPA model. Radiative transfer is calculated to a number of gridpoints (typically 72) in each target tree, which is used to drive the stomatal conductance and photosynthesis submodels. These leaf-level rates are then used to estimate whole-stand water use and carbon uptake (see Sect. "Total canopy transpiration").

an early study on radiative transfer by Norman and Welles (1983), and solidified by Wang and Jarvis, (1990). Since then, many improvements have been made, in particular the leaf gas exchange calculations (Medlyn, 1996, 2004; Medlyn et al., 2007), and the overall organization and dissemination of the code (see http://www.bio.mq.edu.au/maestra/, hereafter referred to as "the MAESTRA website"). Our goal was to widen the applicability of the MAESTRA model by including detailed soil water balance routines and plant hydraulic constraints on gas exchange.

A basic overview of how MAESTRA estimates H_2O and CO_2 exchange is given in Fig. 1. The processes included in the water balance sub-model are illustrated in Fig. 2. A full list of symbols is presented in Appendix A.

The MAESPA model, like MAESTRA and SPA, runs at typically a half-hourly time-step, although it can also be run at hourly or shorter arbitrary time-steps (up to every minute).

2.1.2 Canopy processes

Here, we provide a brief description of the canopy processes represented in MAESPA, which are largely unchanged from the original MAESTRA model (with the exception of stomatal conductance). Our goal is not to provide an in-depth description of the entire MAESTRA model (see Wang and Jarvis, 1990; Medlyn, 2004; Medlyn et al., 2007 and the detailed manual on the MAESTRA website).

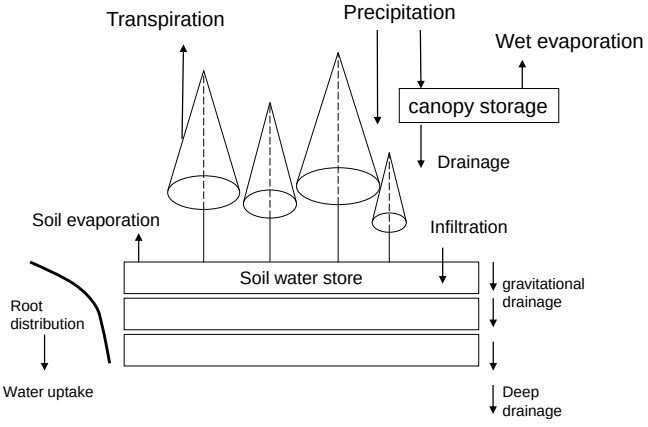

Fig. 2. Flowchart of the water balance components of MAESPA, which are taken from the SPA model. The soil compartment is horizontally homogenous, and vertically divided into an arbitrary number of layers.

Radiative transfer

The radiation routines are described in detail by Wang and Jarvis (1990). The canopy consists of individual tree crowns, which are described by a basic shape (one of several shapes, including ellipsoids, cylinders and cones), length, height to crown base, and width (in x and y directions). Radiation calculations are performed only for a set of target crowns specified by the user (see Sect. "Total canopy transpiration"). A number of grid points are located in a target crown, and radiation (PPFD, NIR and long-wave) at those grid points is

Table 1. Summary of origin of the various components of the MAESPA model. For the many references for the components of the MAESTRA model, see Sects. 2.1.1 and 2.1.2, and the MAESTRA website. For the components taken from SPA, see Williams et al. (2001a, b) for the sources of those components, or the corresponding sections in the main text.

Model component	Source
Radiative transfer	MAESTRA
Leaf energy balance	"
Leaf photosynthesis	"
Stomatal conductance (g_s), leaf and canopy transpiration	"
Additional models for g_s	Tuzet et al. (2003); Medlyn et al. (2011)
Canopy interception	SPA
Soil drainage	"
Soil evaporation	"
Soil surface energy balance	"
Soil temperature profile	"
Soil water balance	"
Infiltration	BROOK90; Federer et al. (2003)
Root water uptake	Modified from SPA; Taylor and Keppler (1975)
Soil water retention and hydraulic conductivity	Campbell (1974)

calculated based on shading within the crown, shading by neighbouring trees, the location of the sun, and whether radiation is direct or diffuse. Scattering of radiation is approximated following Norman (1979). Leaf area within crowns is assumed to be distributed randomly, or to follow a beta-distribution in horizontal and/or vertical directions (Wang et al., 1990). At each grid point, leaf area is separated into sunlit and shaded leaf area (Norman, 1993), and the coupled stomatal conductance – photosynthesis model is run separately for each fraction (Fig. 1).

Photosynthesis

For each grid point in the crown, leaf net photosynthesis is modelled using the standard model of Farquhar et al. (1980).

$$A_\mathrm{n} = \min\left(A_c, A_j\right) - R_\mathrm{d} \quad (1)$$

where A_c is the gross photosynthesis rate when Rubisco activity is limiting, A_j when RuBP-regeneration is limiting, and R_d the rate of dark respiration. A_c and A_j are saturating functions of the intercellular CO_2 concentration (C_i), both of the form $k_1(C_\mathrm{i}\text{-}\Gamma^*)/(k_2 + C_\mathrm{i})$, where Γ^* is the CO_2 compensation point without R_d, and k_1 and k_2 are different parameter combinations for A_c and A_j. The details of these functions and the temperature dependence of the parameters are described elsewhere (e.g. Medlyn et al., 2002).

Stomatal conductance

For each grid point in the crown, leaf-level stomatal conductance to H_2O (g_s) is modelled using a Ball-Berry type approach (Ball et al., 1987) (Eq. 2).

$$g_\mathrm{s} = g_0 + g_1 \frac{A_\mathrm{n}}{C_\mathrm{s}} \times f(D) \quad (2)$$

where A_n is the leaf net assimilation rate ($\mu\mathrm{mol\,m^{-2}\,s^{-1}}$), g_0 the conductance when A_n is zero, g_1 an empirical parameter, $f(D)$ a function of the leaf-to-air vapour pressure deficit (D) and C_s the CO_2 concentration at the leaf surface ($\mu\mathrm{mol\,mol^{-1}}$) (which is corrected for boundary layer effects, but this is usually a small correction).

We have implemented a number of options for the $f(D)$ function, including the Ball-Berry model ($f(D) = 1/\mathrm{RH}$, where RH is relative humidity) (Ball et al., 1987), the Leuning model ($f(D) = 1/(1 + D/D_0)$ (Leuning, 1995), and the model of Medlyn et al. (2011), who showed that $f(D) = 1/\sqrt{D}$ follows from the assumption that g_s varies to maintain $\delta A/\delta E$ constant (cf. Cowan and Farquhar, 1977). The fourth option, which is used in the simulations shown in this paper, is a modified form of the Tuzet et al. (2003) model. This model takes into account the observation that the response of stomatal conductance to D and soil water deficit is controlled by the leaf water potential (Ψ_L) (Comstock and Mencuccini, 1998). Because Ψ_L depends on the soil water potential (Ψ_S) as well as the transpiration rate (which depends on D), Ψ_L summarizes the effect of both D and Ψ_S on g_s (Franks, 2004). Tuzet et al. (2003) use a flexible Ψ_L modifier (in place of the $f(D)$ function in Eq. 2),

$$f_{\Psi_\mathrm{L}} = \frac{1 + \exp[s_f \Psi_f]}{1 + \exp[s_f(\Psi_f - \Psi_\mathrm{L})]} \quad (3)$$

where s_f and Ψ_f are parameters; Ψ_f is a reference water potential, and s_f is the "steepness" of the response of f_{Ψ_L} to Ψ_L. We assume a steady-state in water flow from the soil to the leaf, so that Ψ_L at the gridpoint can be calculated from Ohm's analogy to water transport,

$$E_\mathrm{L} = k_\mathrm{L}\,(\Psi_\mathrm{S} - \Psi_\mathrm{L}) \quad (4)$$

where E_L is the leaf transpiration rate ($\mathrm{mmol\,m^{-2}\,s^{-1}}$), itself dependent on D (and boundary layer effects, see

Sect. "Calculation of leaf temperature and leaf water potential"), and k_L the leaf-specific hydraulic conductance of the soil-to-leaf pathway (see Sect. "Hydraulics of the soil-to-leaf pathway").

Finally, the coupled model of g_s and A can be solved by using the basic diffusion equation,

$$A_n = g_C (C_s - C_i) \quad (5)$$

where g_C is stomatal conductance to $CO_2 (= g_s/1.6)$. The solution of the system of equations (Eqs. 1, 2 and 5) can be written as a quadratic equation, which yields the C_i (see Wang and Leuning, 1998). We solve the Tuzet model (combination of Eqs. 2–5) numerically, by finding the Ψ_L that is the solution both to Eqs. (3) and (4). This way, a unique Ψ_L is calculated for each grid point in the crown. Variation between trees arises due to shading effects, and k_L is allowed to vary from tree to tree (as specified by the user). Also, k_L is either assumed to be constant within the crown, or to follow a function of height above the ground as specified by the user.

It should be noted that Tuzet et al. (2003) used C_i instead of C_a in their model, but we use C_a to be consistent with Medlyn et al. (2011), and to allow for much more straightforward numerical model solution. The argument by Tuzet et al. (2003) to use C_i instead of C_a is that stomata appear to respond to C_i, not C_a (Mott, 1988). However, we note that C_i is still implicit in Eq. (2), because A_n depends on C_i through Eq. (1), and A_n and g_s are coupled by C_i through Eq. (5).

Calculation of leaf temperature and leaf water potential

For the soil water balance, we use the Penman-Monteith equation applied at the canopy level (see Sect. "Total canopy transpiration"), to arrive at consistent calculations for stand energy balance, and boundary layer calculations for soil surface and canopy. At the leaf-level for each grid-point in the crown, transpiration (E_L) is calculated to yield Ψ_L that is the solution to the Tuzet model of stomatal conductance (Eqs. 2 and 3), and to provide estimates of leaf temperature throughout the crown. For each grid point, E_L is calculated with the Penman-Monteith equation (Eq. 6), which takes into account boundary layer effects on the exchange of water vapour between leaves and the surrounding air. An iterative scheme is used that finds the leaf temperature that closes the energy balance of the leaf (following Wang and Leuning, 1998). Full details are provided in Medlyn et al. (2007).

Total canopy transpiration

In MAESPA, the soil water balance is calculated using the spatially-averaged transpiration rate by the stand. This spatial average is calculated for a sample of trees specified by the user (the "target trees"), to limit computing time. An example of a selection of target trees is given in Fig. 3. We have chosen not to simulate spatial variation in soil water content based on water uptake of the single trees in a stand, because such a model would be very difficult to parameterize and test.

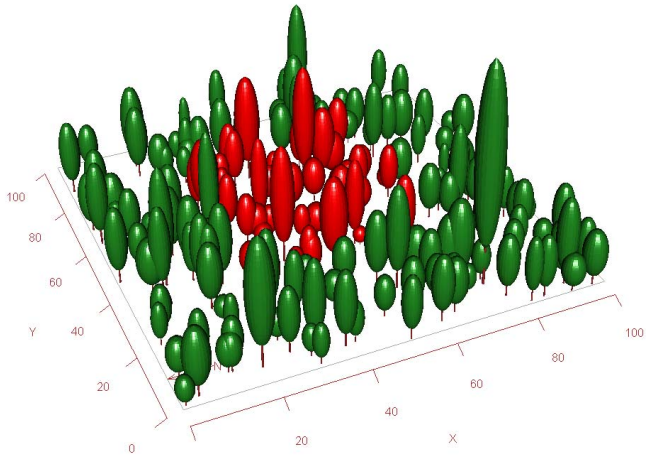

Fig. 3. Example of a stand of trees as represented in the MAESPA model. Water use and carbon uptake are calculated for a sample of target trees, here shown in red, and then added to give the totals for the stand. It is recommended to select a set of target trees that are representative of the stand, and to account for edge effects.

This approach requires that we scale up estimates of transpiration to the stand level, and estimate total global (shortwave + longwave) radiation reaching the forest floor (for the soil heat balance calculations, see Sect. 2.1.4). Absorbed radiation (photosynthetically active radiation (PAR), near-infrared radiation (NIR) and thermal) is summed for each tree, and corrected for the difference in leaf area per tree for the sample trees, and that for the entire stand. Using the stand density, estimates of global radiation ($W\,m^{-2}$) incident on the soil surface are obtained. Next, the average whole-tree conductance ($mol\,tree^{-1}\,s^{-1}$) is calculated across the sample trees (weighed by their total leaf areas), and once again corrected for the difference in tree leaf area between sample trees, and the average tree in the entire stand. Stand transpiration is re-calculated using this average canopy conductance, and the intercepted radiation per tree, using the Penman-Monteith equation,

$$\lambda E_T = \frac{s R_n + D g_B c_p M_a}{s + \gamma g_B / g_V} \quad (6)$$

where λ the latent heat of water vapour ($J\,mol^{-1}$), E_T is canopy transpiration ($mol\,m^{-2}$ (ground) s^{-1}), s the slope of the relation between saturation vapour pressure and temperature ($Pa\,K^{-1}$), R_n net radiation ($W\,m^{-2}$), g_B the boundary layer conductance, and g_V the total conductance to water vapour. The boundary layer conductance (g_B, $mol\,m^{-2}\,s^{-1}$) for the canopy is calculated following Jones (1992),

$$g_B = \frac{c \times k_V^2 \times u_z}{[\log((z_H - z_D)/z_0)]^2} \quad (7)$$

where k_V von Karman's constant, u_z the wind speed measured at a height of z_H, and c converts to molar units. The parameters z_D and z_0 are related to the extinction of wind speed above and within the canopy: z_0 is the "roughness length" related to the roughness of the canopy surface, and z_D is a reference height. Both these parameters may be estimated from canopy height (Jones, 1992, p. 68), or from more detailed methods that account for stand structure (Schaudt and Dickinson, 2000).

The total conductance to water vapour is,

$$g_V = 1/(\frac{1}{g_C} + \frac{1}{g_B}) \quad (8)$$

where g_C the canopy conductance (mol m^{-2} s^{-1}), which is estimated by averaging total conductance (mol tree^{-1} s^{-1}) across the sample trees weighed by their total leaf areas, and multiplying by stand density (m^{-2}).

2.1.3 Water balance

Overview

The soil water balance is calculated for a horizontally homogenous soil compartment, separated vertically in a number of layers (typically ca. 10, specified by the user). The advantage of a multi-layer soil model is that the root density distribution can be specified, as well as vertical variation in soil texture. Furthermore, experiments have shown that plant water potential tends to equilibrate with the wettest zones in the soil, not the average soil water potential (Schmidhalter, 1997). Only a multi-layer soil model can reproduce this observation.

In MAESPA, the soil water storage in each of the horizontally homogenous layers (s_i, mm) is calculated from infiltration (I_i), drainage (D_i), root water uptake (E_i) and soil evaporation ($E_{s,i}$) (Eq. 9), at the same time-step as the aboveground processes (typically, half-hourly). Soil evaporation draws water only from the top layer. Drainage out of the lowest root layer is defined as deep drainage.

$$\frac{ds_i}{dt} = I_i - E_i - D_i \text{ for } i>1, \text{ and}$$
$$\frac{ds_i}{dt} = I_i - E_i - D_i - E_{s,i} \text{ for layer 1.} \quad (9)$$

Infiltration

The rain that reaches the soil surface is assumed to infiltrate into more than just the top layer. This is accounting for rapid soil water flow through macropores (accounting for increases in soil water content at depth after heavy rainfall that cannot be accounted for by matric drainage rates). We use a simple exponential function (taken from the BROOK90 model, (Federer et al., 2003) (Eq. 10).

$$\text{For } i = 1,\ I_i = P_u \times (z_i/Z)^{\phi}$$
$$\text{For } i>1,\ I_i = P_u \times \left(\left((\sum_1^i z_i)/Z\right)^{\phi} - \left((\sum_1^{i-1} z_i)/Z\right)^{\phi}\right) \quad (10)$$

where ϕ is an infiltration parameter (0-1), z_i the depth to the bottom of layer i (m), and Z the total soil depth (m). If $\phi = 0$, all infiltration occurs in the top soil layer (no macropore flow). If $\phi = 1$, all layers receive equal infiltration.

Root water uptake

Total water uptake is distributed among soil layers according to the fine root density and soil water potential in those layers. The fraction of roots in each layer can be specified manually, or assumed to follow Eq. (11), which is useful because Jackson et al. (1996) have summarized a large database on root distributions with this equation.

$$F_R = (1 - \beta^{100 \cdot z_i})/(1 - \beta^{100 \cdot Z}) \quad (11)$$

where F_R is the cumulative fraction of fine roots to depth z (m), and β is a parameter that specifies the shape of the distribution (see Jackson et al., 1996). Soil depth is multiplied by 100, to be consistent with Jackson et al. (1996) who specified z in cm. We have modified the original equation so that the total fine root length (an input parameter) is reached at the maximum depth of the rooting profile.

The root system can be viewed as a combination of resistances that are coupled in parallel, consisting of a soil-to-root surface resistance (R_{sr}) and a resistance to water uptake by the root itself (the radial resistance, R_{rad}). Because water transport is largely passive, following gradients in water potential from soil to roots, the relative water uptake by different layers in the soil follows from the partitioning of the resistances to water uptake in these layers. Generally, water uptake in a soil layer (E_i) is,

$$E_i = (\Psi_{S,i} - \Psi_{R,i})/(R_{sr,i} + R_{rad,i} + R_{lg,i}) \quad (12)$$

where $\Psi_{S,i}$ is the soil water potential in layer i, $\Psi_{R,i}$ is the root xylem water potential, R_{sr} the soil-to root resistance, R_{lgi} the longitudinal resistance to water flow, and R_{rad} the radial resistance to water uptake (across the root epidermis to the xylem). This is a very difficult equation to solve simultaneously for multiple soil layers, because $\Psi_{R,i}$, R_{rad} and R_{lg} are typically unknown, and could vary with depth of the layer (especially $R_{lg,i}$, as the path length through the root becomes longer). To solve Eq. 12, we follow the assumptions by (Taylor and Keppler, 1975) who showed in an elegant experiment that (1) R_{lg} is very small compared to R_{rad}, so that $\Psi_{R,i}$ can be taken as a constant, and (2) R_{sr} is small compared to R_{rad}, except in very dry soil. Because R_{rad} is inversely proportional

to the total fine root length in a soil layer, it follows that,

$$E_i \propto L_{\mathrm{v},i}\left(\Psi_{\mathrm{S},i} - \overline{\Psi_{\mathrm{R}}}\right) \quad (13)$$

where $\overline{\Psi_{\mathrm{R}}}$ is a mean root water potential, and $L_{\mathrm{v},i}$ the fine root density ($\mathrm{m\,m^{-3}}$) in layer i. The constant of proportionality may be found from the fact that $\sum E_i = E_{\mathrm{T}}$, where E_{T} is the total water uptake. Note that we do include R_{sr} in the calculations of the overall resistance of the soil-to-leaf pathway (see Sect. "Hydraulics of the soil-to-leaf pathway"), but omit it here to simplify the *fractional* uptake of water from different soil layers. The mean root water potential is taken as the minimum value allowed for roots (Ψ_{Rmin}), an input parameter; so that no uptake is possible in soil layers where the soil water potential is lower than Ψ_{Rmin}). When $\Psi_{\mathrm{R}} > \Psi_{\mathrm{S}}$, it is assumed that water does not flow from roots back into the soil, that is, we do not consider hydraulic redistribution in our model (see Domec et al., 2012).

Soil evaporation

The evaporation of water from the soil surface is estimated with a physical-based model developed by Choudhury and Monteith (1988), and modified by Williams et al. (2001a). Soil evaporation draws water only from the top layer, and assumes that water has to travel through a thin dry layer at the soil surface.

The rate of evaporation (mm) is determined from the difference between water vapour pressure in the soil pore space and the air above, and a conductance to vapour transfer (Eq. 14),

$$E_{\mathrm{s}} = G_{\mathrm{s,t}} k_1 \left(e_{\mathrm{s}} - e_{\mathrm{a}}\right) \quad (14)$$

where $G_{\mathrm{s,t}}$ is the total conductance from the soil air space to the air above the boundary layer ($\mathrm{m\,s^{-1}}$), e_{a} the partial water vapour pressure of the air (kPa), and e_{s} that of the soil pore space (kPa). The term k_1 converts from pressure units to volumetric units. $G_{\mathrm{s,t}}$ is the total conductance, including the path through the soil (G_{ws}), and that through the boundary layer just above the soil surface (G_{am}). The latter is estimated following Eq. (7) (Sect. "Total canopy transpiration"), with the reference height z_{D} set to zero. Next, G_{ws} is estimated from the diffusivity of water vapour, which is soil temperature dependent, and the tortuosity of the soil air pathway, which determines the effective path length for vapour transfer.

$$G_{\mathrm{ws}} = D_{\mathrm{eff}}\left(\theta_1 / L_{\mathrm{d}}\right) \quad (15)$$

$$D_{\mathrm{eff}} = \omega_s \theta_1 D_{\mathrm{w}} \quad (16)$$

where D_{eff} is the effective diffusivity, ω_s a tortuosity parameter, θ_1 the pore fraction of the top soil layer, L_{d} the thickness of the dry layer at the soil surface, and D_{w} diffusivity of water vapour (calculated following Jones (1992) accounting for soil temperature). The rationale for Eq. (15) (Choudhury and Monteith, 1988) is that G_{ws} is proportional to the air space in the soil, but inversely proportional to the distance water vapour has to travel. This distance is a function of both the thickness of the dry layer (L_{d}), and the tortuosity of the dry layer (Eq. 16). L_{d} depends on the timing of the last rainfall, and the rate of soil evaporation, but is not affected by plant water uptake. Following Williams et al. (2001b), MAESPA keeps track of multiple dry layers to account for complex dynamics with short intermittent storms. A minimum value ($L_{\mathrm{d,min}}$) is specified as a parameter to prevent very high rates of soil evaporation in wet soil.

The partial pressure of water vapour in the soil pore space is calculated from,

$$e_{\mathrm{s}} = e_{\mathrm{sat}} \times \exp\left\{\Psi_{\mathrm{s},1} V_{\mathrm{w}} / \left(R T_{\mathrm{s}}\right)\right\} \quad (17)$$

where e_{sat} is the saturated vapour pressure (calculated from temperature following Jones 1992), $\Psi_{\mathrm{s},1}$ the soil water potential in the surface layer, V_{w} the partial molal volume of water ($\mathrm{m^3\,mol^{-1}}$), R the gas constant, and T_{s} the soil surface temperature (K).

Canopy interception

The Rutter et al. (1975) model of canopy rainfall interception is used. Rain has two possible fates: (1) it falls through the canopy without being intercepted or (2) it gets intercepted by the canopy, where it adds to a pool of canopy water, that slowly drains. If the maximum canopy pool is reached, all additional rainfall in that time-step drains immediately. Water also evaporates from the wet canopy, determined by the Penman-Monteith equation (see Sect. "Total canopy transpiration"), using infinite canopy conductance (because free water is available), but with VPD set to a very low value.

The change in canopy water storage (W_{can}) is given by,

$$\frac{\mathrm{d}W_{\mathrm{can}}}{\mathrm{d}t} = (1 - r_1)\,P - E_{\mathrm{w}} - e^{r_2 + r_3 W_{\mathrm{can}}} \quad (18)$$

where E_{w} the wet evaporation rate ($\mathrm{mm\,t^{-1}}$), r_1 the free throughfall fraction (0–1), and r_2 and r_3 are canopy drainage parameters. This differential equation is integrated with a Runge-Kutta method to obtain canopy throughfall, canopy storage, and wet evaporation rates.

Drainage

The vertical drainage of soil water is estimated directly from the soil hydraulic conductivity, which itself is a function of the soil water content. After adding the infiltration of rainfall to the soil water content for each layer, the water balance for each soil layer becomes,

$$\frac{\mathrm{d}W_{\mathrm{i}}}{\mathrm{d}t} = D_{i-1}\left(\theta_{i-1}\right) - D_i\left(\theta_{\mathrm{i}}\right) \quad (19)$$

where D_i is the drainage from layer i. Because water is assumed to not travel upwards in the soil, this equation can be

solved for one layer at a time, starting at the top and moving downward. Drainage is simply equal to the soil hydraulic conductivity ($m\,s^{-1}$) in that layer, which is calculated from θ_i. The system of equations is solved with a Runge-Kutta integrator (following the SPA model, Williams et al., 2001a, b).

Hydraulics of the soil-to-leaf pathway

We use the simple set of equations developed by (Campbell, 1974) for the dependence of soil water potential and the hydraulic conductivity on the soil water content. Soil water potential (Ψ_S, MPa) is given by Eq. (20),

$$\Psi_s = \Psi_e \left(\frac{\theta}{\theta_{sat}} \right)^{-b} \quad (20)$$

where θ the soil volumetric water content ($m^3\,m^{-3}$), θ_{sat} the soil porosity, and Ψ_e and b are soil texture dependent parameters (see Cosby et al., 1984). Each of these parameters can vary by soil layer (i subscripts are omitted for clarity). The soil hydraulic conductivity is estimated from Eq. (21),

$$K_s(\Psi_s) = K_{sat} \left(\frac{\Psi_e}{\Psi_s} \right)^{2+3/b} \quad (21)$$

where K_s the conductivity ($mol\,m^{-1}\,s^{-1}\,MPa^{-1}$), Ψ_e and b are the same parameters as in Eq. (20) (using the fact that conductivity and water potential are physically related), and K_{sat} is the saturated hydraulic conductivity ($mol\,m^{-1}\,s^{-1}\,MPa^{-1}$).

The soil-to-root resistance ($MPa\,s\,m^2\,(ground)\,mol^{-1}$) is estimated with the single root model of Gardner (1960) (see Williams et al., 2001a and Duursma et al., 2008 for more details). This model estimates the effective path length for water transport through the soil matrix to the root surface from the fine root density. The equation is,

$$R_{sr,i} = \frac{\log(\frac{r_s}{r_r})}{2\pi L_V H_s K_s} \quad (22)$$

where r_r the mean root radius (m), L_v the total fine root density ($m\,m^{-3}$) in the soil layer, H_s the height of the soil layer, and r_s the mean distance between roots ($1/\sqrt{\pi L_V}$). The total resistance for all soil layers combined ($R_{sr,t}$) is estimated by assuming that the resistances are coupled in parallel. The total leaf-specific hydraulic conductance (k_L, $mmol\,m^{-2}\,(leaf)\,s^{-1}\,MPa^{-1}$) from soil to leaf can now be found as,

$$k_L = 1/(\frac{1}{k_P} + R_{sr,t} \times L_T) \quad (23)$$

where L_T total canopy leaf area index ($m^2\,(leaf)\,m^{-2}\,(ground)$), and k_P the plant component of the leaf-specific hydraulic conductance ($mmol\,m^{-2}\,s^{-1}\,MPa^{-1}$), which is typically estimated from measurements of E_L and Ψ_L under well-watered conditions (see, e.g. Delzon et al., 2004). It is assumed that k_P includes the root components of the plant pathway (defined in Eq. 12 by the resistances R_{rad} and R_{lg}), and that these components do not change with the plant water potential.

Following Williams et al. (2001a), we calculate a weighted soil water potential for use in the calculation of Ψ_L and stomatal conductance. The Ψ_s in each layers is weighed by the maximum water transport possible in that layer, depending on R_{sr} in that layer and a minimum root water potential ($\Psi_{R,min}$),

$$\Psi_S = \frac{\sum_{i=1}^{N} \Psi_{S,i} \times E_{max,i}}{\sum_{i=1}^{N} E_{max,i}} \text{ where } E_{max,i} = (\Psi_{S,i} - \Psi_{R,min})/R_{sr,i}. \quad (24)$$

2.1.4 Soil heat balance

Overview

The components of the soil surface heat balance are calculated to arrive at the soil surface temperature, and the vertical gradient of soil temperature. The soil surface temperature affects only the soil evaporation (see Sect. "Soil evaporation"). If soil evaporation is not of interest, or can be assumed negligible, the soil heat balance need not be calculated (thereby simplifying the parameterization).

Soil surface temperature

The soil energy balance is the sum of four heat fluxes: net radiation (Q_n), soil surface evaporation (latent heat flux) (Q_e), soil heat transport (to deeper soil layers) (Q_c) and sensible heat flux (Q_h). Due to conservation of energy, these fluxes sum to zero at any time:

$$Q_n + Q_e + Q_c + Q_h = 0. \quad (25)$$

All the components in Eq. (25) depend on the soil surface temperature ($T_{s,1}$). The MAESPA model finds the soil surface temperature that provides closure in the soil energy balance.

Net radiation on the soil surface (Q_n) is global radiation (solar + downward thermal) minus long-wave radiation (Q_L) emitted by the soil surface. The latter depends on the soil surface temperature (Eq. 26).

$$Q_L = \varepsilon \sigma T_s^4 \quad (26)$$

where ε is the emissivity (assumed to equal 0.95), σ the Stefan-Boltzmann constant ($W\,m^{-2}\,K^{-4}$) and T_s is in K. Global down-welling radiation is the sum of short-wave radiation (i.e. solar radiation minus that intercepted by the canopy), and long-wave radiation emitted by the canopy.

The soil latent heat flux (Q_e) is calculated from soil evaporation (see Sect. "Soil evaporation"), and the latent heat of evaporation (a function of temperature; Jones, 1992).

Soil heat transport (Q_c) follows from the difference in soil temperature between the first and second layer,

$$Q_c = K_{\mathrm{th}} \left(T_{\mathrm{s},2} - T_{\mathrm{s},1}\right) / \Delta z_{1,2} \quad (27)$$

where K_{th} is the the soil thermal conductivity ($\mathrm{W\,m^{-1}\,K^{-1}}$, see Sect. "Soil surface temperature"), and $\Delta z_{1,2}$ the depth difference between the second and first layer (m).

Sensible heat flux (Q_{h}) is calculated from the difference between air temperature and soil surface temperature, and the total conductance to heat (Eq. 28)

$$Q_{\mathrm{h}} = c_p \rho G_{\mathrm{a,m}} \left(T_{\mathrm{s},1} - T_{\mathrm{air}}\right) \quad (28)$$

where c_p the heat capacity of air ($\mathrm{J\,kg^{-1}\,K^{-1}}$, a constant), ρ the (temperature-dependent) density of air ($\mathrm{kg\,m^{-3}}$), $G_{\mathrm{a,m}}$ the boundary layer conductance to heat transfer (assumed to be equal to that of water vapour transfer, see Sect. "Soil evaporation"), and $T_{\mathrm{s},1}$–T_{air} the temperature gradient between soil surface and the air.

Soil temperature profile

The transport of heat down the soil temperature gradient is calculated following the SPA model (Williams et al., 2001b). The Fourier heat transport equation is solved using the Crank-Nichols scheme (Press et al., 1990) resulting in a soil temperature profile and corresponding heat fluxes between soil layers. Inputs for this routine are the soil thermal conductivity (by layer), and soil heat capacity.

We used an empirical model developed by Lu et al. (2007) to estimate the soil thermal conductivity (in $\mathrm{W\,m^{-1}\,K^{-1}}$) from soil porosity, water content, temperature and organic matter content. Their model takes slightly different parameter values for fine and coarse textured soils; we used the soil texture parameter (b in Eq. 20) to determine which parameter set to use (based on their Table 1, we used $b = 5.3$ below which soils are considered "coarse textured"). With this method, it is straightforward to set the top layer of the soil as a "litter layer" that effectively insulates the soil through a very low thermal conductivity.

The heat capacity of the soil is determined by separating the soil into solid (quartz) and water fractions, and finding the weighted average of their heat capacities (cf. de Vries, 1963; see also Ogée et al., 2001), and assuming that the soil air fraction has negligible heat capacity.

2.2 Parameterization

In MAESPA, the water balance is calculated for a horizontally homogenous soil, but the canopy consists of a collection of single trees. Canopy transpiration is estimated based on transpiration by the "sample trees", and it is therefore vital that these sample trees represent the canopy in terms of water use. It is recommended that MAESPA is run for a large number of sample trees, for example in an arrangement shown in Fig. 3. For all trees in the stand, estimates of leaf area, crown shape, crown width, crown length and height to crown base are needed. Stands may also consist of just one tree, in which case the product of plot size and rooting depth can be interpreted as the soil volume, or pot volume, available to the tree.

Environmental drivers need to be specified on a (half-)hourly time-step, and include air temperature, solar radiation, precipitation, relative humidity and optionally wind speed and CO_2 concentration. For the water balance, crucial parameters are total rooting depth and the soil water retention curve. The latter can be estimated from soil texture, and equations summarized by e.g. Saxton and Rawls (2006) and Cosby et al. (1984). A brief summary of the list of parameters needed to run the water balance component of MAESPA is given in Table B1.

2.3 Implementation and batch utility

MAESPA is written in Fortran, with simple text-based input and output files. An R (R Development Core Team, 2011) package is available, *Maeswrap*, which aides sensitivity analysis and other computer-intensive simulation studies. This also includes a utility to graph the stand in 3-D (Fig. 3 was produced with the *Maeswrap* package). The compiled model and the source code are available on the MAESTRA website (see Sect. 2.1).

2.4 Application of MAESPA: a case study on the interaction between C_{a} and drought

In the following, we present three brief case studies that illustrate the application of the MAESPA model to studying complex interactions between environmental drivers and plant parameters. All case studies analyse the interaction between atmospheric CO_2 concentration (C_{a}) and drought.

2.4.1 Dry-down simulations

We simulated the response of several plant variables to a dry-down in order to establish a clear picture of the baseline expectation of the interaction between C_{a} and drought, that is, the interaction when C_{a}-related feedbacks and acclimation are ignored. We used a hypothetical stand with total leaf area index of $3.8\,\mathrm{m^2\,m^{-2}}$, with a default leaf physiology parameter set (see Table 2 for parameters and their values), and the Tuzet model of stomatal conductance (Eqs. 2 and 3). Ambient C_{a} was set to 380 ppm, and elevated C_{a} was chosen as 620 ppm (Barton et al., 2010). Weather data was generated for a typical sunny summer day, using the Bristow and Campbell algorithm (Bristow and Campbell, 1984), and was the same for each day during the dry down, as was the solar angle (although it did change during the day).

Table 2. Important parameters for the simulation of a dry-down on daily whole-plant gas exchange and plant water relations. The soil type was a loamy sand (parameters from Cosby et al., 1984). Half-hourly weather data were estimated from daily T_{air} amplitude.

Parameter	Value
Number of soil layers	10
Root distribution (β)	0.98
B	4.3
Ψ_e	-0.35 kPa
K_{sat}	200 mol m^{-1} s^{-1} MPa^{-1}
g_0	0.01 mol m^{-2} s^{-1}
g_1 (Tuzet model)	4.5
s_f	3.2 MPa^{-1}
Ψ_f	-1.9 MPa
k_p	2 mmol m^{-2} s^{-1} MPa^{-1}
J_{max}	150 µmol m^{-2} s^{-1}
V_{cmax}	90 µmol m^{-2} s^{-1}
Tree leaf area	35 m^2
Stand density	1100 trees ha^{-1}
Daily max. D	3.0 kPa
Daily $T_{max} - T_{min}$	10–30 °C
C_a	380 ppm
Wind speed	0.5 m s^{-1}

2.4.2 Effect of acclimation of leaf parameters on C_a × drought interaction in water use and CO_2 uptake

Acclimation of leaf physiology to long-term growth at eC_a is one possible explanation for why many real-world experiments deviate from baseline expectations of $C_a \times$ drought interactions. We test the impact of acclimation of two leaf physiology parameters, k_L and Ψ_f. A number of studies have found decreases in the leaf-specific hydraulic conductance (k_L) in plants grown in eC_a (Atkinson and Taylor, 1996; Eamus et al., 1995; Eguchi et al., 2008; Heath et al., 1997), with reductions in a wide range of 10–100 %.

Berryman et al. (1994) found a higher sensitivity of g_s to decreasing water content of excised leaves in *Maranthes corymbosa*, which can be interpreted as a less negative Ψ_f in the Tuzet model (Eq. 3). This observation is also consistent with a higher sensitivity to abscisic acid (ABA) in eC_a found in a number of species (Dubbe et al., 1978; McAdam et al., 2011), and the fact that ABA concentrations increase in low Ψ_L (Pierce and Raschke, 1981).

To test the sensitivity of the $C_a \times$ drought interaction to these parameters, we ran two additional dry-down simulations, one with a 50 % reduction in k_L at eC_a, and one with a 0.4 MPa increase in Ψ_f. Both these changes in parameter values are within observed ranges of change with long-term growth at eC_a, but are arbitrary and only chosen to illustrate the effect on the $C_a \times$ drought interaction. All other settings and parameters were as specified in the dry-down simulation (Sect. 2.2.1).

2.4.3 Drought × C_a interaction in cherry seedlings

To illustrate the importance of whole-plant feedbacks in treatment responses, we applied the model to a $C_a \times$ drought experiment. Centritto et al. (1999a, b) describe an experiment where cherry seedlings were grown in ambient C_a concentration (aC_a) (350 ppm) and elevated C_a (eC_a; 700 ppm) treatments in well-watered conditions until half the plants were subjected to a dry-down. The analysis of their results was complicated by the fact that total leaf area of eC_a seedlings was higher than that of aC_a seedlings, compensating for lower water use per unit leaf area, so that total water use was similar between treatments. We re-analysed their dataset in a model-based framework where we can integrate effects of leaf area, C_a, and leaf-level physiology parameters on whole-plant interactions between C_a and drought.

We estimated MAESPA parameters for the cherry seedling based on the published information as much as possible, and found the remaining parameters by fitting to observed data (see below). Details and estimated parameters are presented in Table 3. We constructed a weather dataset based on the latitude of the study and the reported mean air temperature and relative humidity. Daily incident PAR was estimated from air temperature using the Bristow and Campbell algorithm (Bristow and Campbell, 1984). Using the fitted parameter set for aC_a plants, we simulated water use by the eC_a plants, with the only difference that leaf area was increased as observed in the experiment.

3 Results

3.1 The interaction between C_a and drought

A simulation was carried out to establish baseline behaviour of MAESPA during a dry-down.

At ambient C_a, simulated total water use (E_T) declines earlier and more rapidly than total carbon uptake (A_T) (Fig. 4a and b), implying that C_i/C_a declines (Fig. 4c) and A_T/E_T increases as the dry-down progresses (Fig. 4d). As the soil water content declines (Fig. 4e), midday leaf water potential (Ψ_L) decreases steadily, and continues to decrease because of cuticular water loss (Table 2). As g_s decreases during the dry-down, the difference between leaf and air temperature increases (Fig. 4g), and the depth of water uptake gradually shifts to deeper layers (Fig. 4h).

These simulations also summarize our baseline expectations, in the absence of feedbacks or acclimation, for a $C_a \times$ drought interaction. Under eC_a, E_L is initially lower (Fig. 4a), which leads to less negative Ψ_L (Fig. 4f), and a higher soil water content (Fig. 4e). The daily integrated transpiration efficiency (A_T/E_T) is higher under eC_a, and increases more rapidly under eC_a as compared to aC_a (Fig. 4d). This latter prediction is sensitive to the assumed value for g_0 (the cuticular conductance), so that a lower g_0 leads to

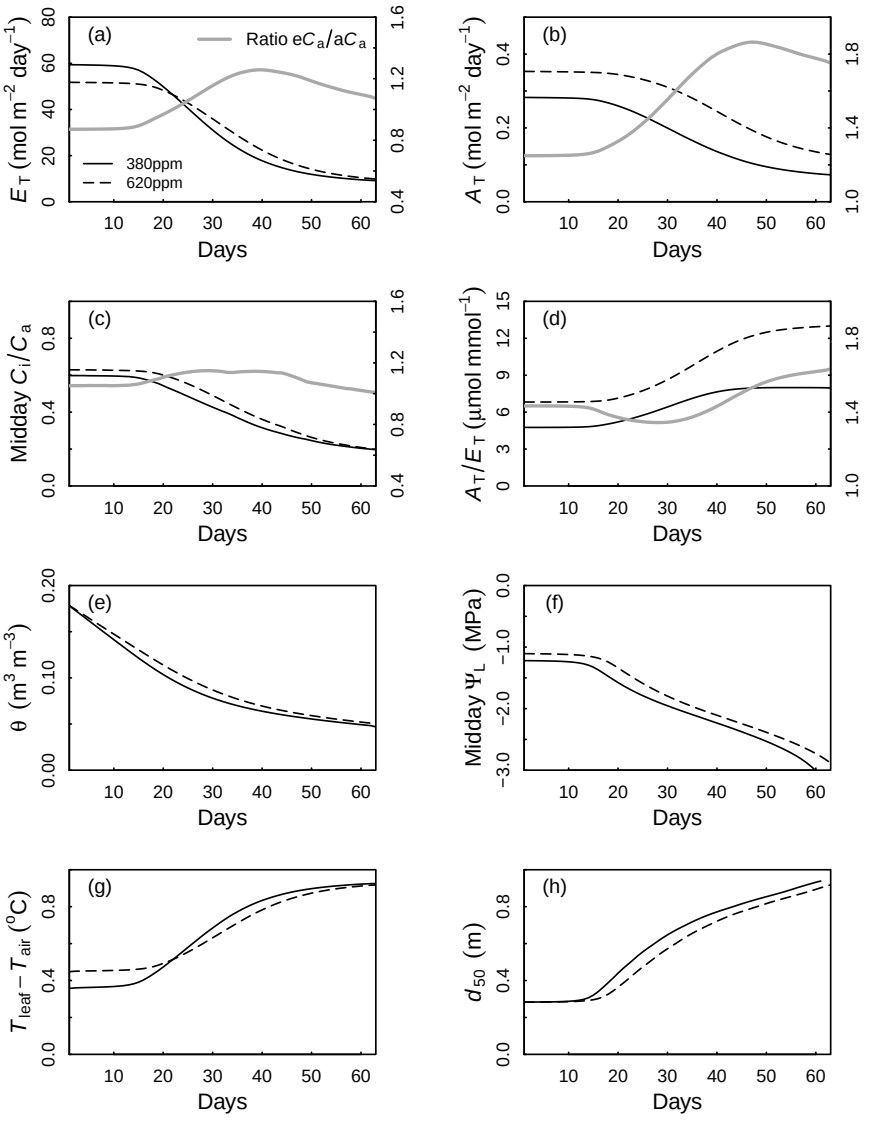

Fig. 4. Simulation of the effect of a dry-down on whole-plant fluxes and water balance under ambient and elevated C_a. The simulation was performed for a single tree with 35 m^2 leaf area in a stand of identical trees. Fluxes are expressed as averages over the canopy of that single tree. See Table 1 for the parameter set used in the simulation. Shown are the decrease in total water use (E_T), total daily net photosynthesis (A_T), midday C_i/C_a, the daily integrated transpiration efficiency (A_T/E_T), volumetric soil water content (θ), midday leaf water potential for the sunlit leaves (Ψ_L), the difference between leaf and air temperature (T_{leaf}–T_{air}), and the depth of root water uptake (d_{50}, the depth above which 50 % of water is taken up). For panels **(a)–(d)**, the ratio of eC_a to aC_a is shown with a grey line. Note the difference in scale for this ratio (right y-axis) for panel **(b)**.

a more pronounced increase in A_T/E_T as the drought progresses (not shown). Both E_T and A_T show a three-phase response when expressed as the ratio eC_a to aC_a (Fig. 4a and b). At first, when both plants have sufficient water, the ratio is constant. The ratio then increases due to higher soil water content in the eC_a treatment. When this saved water store is exhausted (by day 40–45), the ratio declines, as both E_T and A_T are increasingly controlled by the cuticular conductance.

MAESPA predicts a strong positive interaction between C_a and drought for two reasons. The first is the "water savings" effect described above: photosynthesis of elevated C_a trees is high for longer due to higher soil moisture. Secondly, even when both treatments are at the same soil water content, photosynthesis is stimulated more by eC_a in dry soil compared to wet soil (Fig. 5a, see also Fig. 4). This response arises because C_i declines as the soil dries out (Fig. 4c), and A_n is more sensitive to C_i at low values of C_i, due to the saturating response of A_n to C_i. This "C_i effect" is demonstrated in Fig. 5a (solid line).

Table 3. Important parameter settings for the simulation of the $C_a \times$ drought interaction in cherry.

Parameter	Value	Source
Pot volume	6.6 dm^3	
Leaf area (start–end)	0.06–0.08 m^2 (aC_a), 0.1–0.115 m^2 (eC_a)	Calculated from Centritto et al. (1999a), their Table 5 and Fig. 7
C_a	350 (aC_a), 700 (eC_a)	
V_{cmax} at 25 °C	50 µmol m^{-2} s^{-1}	Estimated by visually fitting Eq. (1) to Fig. 3 in Centritto et al. (1999b)
J_{max}, at 25 °C	100 µmol m^{-2} s^{-1}	As above
b	4.3	Loamy sand
Ψ_e	−0.35 kPa	Loamy sand
θ_{sat}	0.6 m^3 m^{-3}	Typical value
Ψ_f	−2.3 MPa	Fitted
s_f	2.2 MPa^{-1}	Fitted
g_1 (Tuzet model)	5.5	Fitted
k_P	1.35 mmol m^{-2} s^{-1} MPa^{-1}	Fitted
Ψ_{Rmin}	−3 MPa	Assumed value
β	0.99	Typical value; Jackson et al. (1996)

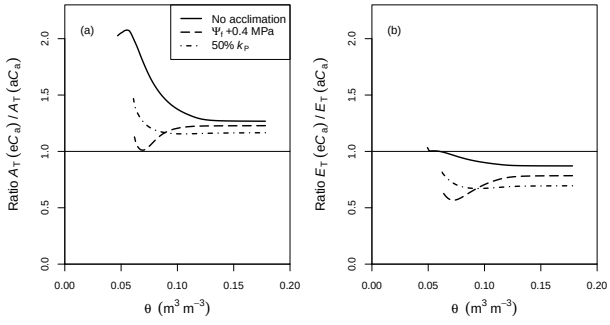

Fig. 5. Illustration of the influence of acclimation on the interaction between C_a and drought. Panel **(a)**, relative C_a effect on total canopy CO_2 uptake (A_T) as a function of soil water content (θ) during a simulated dry-down. Panel **(b)** shows total canopy transpiration rate (E_T) for the same simulations. The solid line shows the interaction when all plant parameters are unchanged due to growth at eC_a ("no acclimation"). Note that in very dry soil, transpiration rates are similar in aC_a and eC_a, but the stimulation of A_T due to eC_a is much higher than in wet soil (a positive interaction of drought and eC_a). These effects are much reduced for a higher sensitivity to Ψ_L in the stomatal conductance model ("$\Psi_f + 0.4$ MPa"), which leads to a negative interaction between C_a and drought (the C_a effect is less in dry soil than wet soil, for both E_T and A_T). A lower plant hydraulic conductance (k_P) reduces E_T in wet soils, and greatly reduces the positive interaction of C_a and drought that was found without acclimation.

We studied the effect of acclimation of two leaf physiology parameters, the leaf-specific hydraulic conductance (k_P) and the sensitivity to Ψ_L (Ψ_f, Eq. 3), on the "C_i effect". When k_P is reduced by 50 %, the strong positive interaction with soil water content as observed in the baseline simulation is much reduced (Fig. 5a), so that the eC_a stimulation of A_T is only moderately dependent on soil water content. When Ψ_f is increased by 0.4 MPa, the interaction even reversed, so that A_T decreases with eC_a in very dry soil (Fig. 5a) and E_T is reduced by eC_a in very dry soil (Fig. 5b). This occurs because a higher Ψ_f leads to reduced stomatal conductance in eC_a compared to aC_a as the Ψ_L declines in dry soil.

Plant size may change following long-term growth at eC_a, which can feed back to drought responses and modify $C_a \times$ drought interactions. We simulated a $C_a \times$ drought interaction in an experiment where plant leaf area increased in response to eC_a, fully compensating the lower water use per unit leaf area. MAESPA was able to simulate the decrease in soil water content and Ψ_L (Fig. 6a and b), after calibrating parameters related to stomatal conductance (Table 3) using the aC_a treatment only. Using this parameter set, however, the measured Ψ_L was overestimated early in the dry-down for the eC_a treatment, and underestimated late in the dry-down (Fig. 6b). The relative response of E_T to eC_a (Fig. 6) illustrates that the eC_a plants used more water early in the dry-down, which led to a more severe water stress, so that water use was substantially less under eC_a towards the end of the dry-down. This response was also predicted by MAESPA

(Fig. 6c), because Ψ_L was lower in the (simulated) eC_a treatment.

Using the calibrated model, it is possible to tease apart contributions of different mechanisms on the overall interaction between C_a and drought, by running simulations with different settings. For this experiment, we ran simulations exploring the contributions of changes in leaf area vs. changes in leaf-level water use. If plant leaf area was assumed unchanged between aC_a and eC_a treatments, we observed a very strong positive interaction between C_a and drought on E_T, as expected from the baseline simulations (Fig. 6c, dashed line). If leaf area was assumed to increase in the eC_a treatment, but leaf-level water use was assumed not to change (dot-dashed line in Fig. 6c), E_T declined much more quickly, indicating that the leaf-level response to eC_a did have a substantial ameliorating effect on the response of E_T to drought.

Finally, we quantified the drought impact on total photosynthesis in the cherry experiment, by calculating total photosynthesis over the entire dry-down under different assumptions, and expressing it relative to simulated total photosynthesis under well-watered conditions (Fig. 7). At aC_a, drought reduced total photosynthesis by 22 %. For the eC_a treatment, three simulations are summarized. The first two are calculated drought responses if leaf area is the same between aC_a and eC_a treatments, and the third is the model prediction for the actual experimental conditions of the cherry experiment. The first simulation, Run 1, is the "baseline", which includes both the "water savings" and the "C_i effect" (see above). The second simulation, Run 2, is at aC_a, but with reduced leaf area to match the pre-drought eC_a water use, and therefore is equivalent to the water savings effect of eC_a. In the third simulation, Run 3, leaf area was increased similarly as in the cherry experiment, so that pre-drought water use was the same as in the aC_a. In the eC_a simulations, drought reduced total photosynthesis by 10 % (without feedbacks; Run 1), and 13 % (Run 2, water savings only), respectively. With the leaf area feedback (Run 3), there was a larger reduction in total photosynthesis (30 %), which counteracted the positive interaction between C_a and drought. In summary, there was a positive eC_a × drought interaction, because drought reduced photosynthesis less in eC_a than in aC_a. This positive interaction was largely the result of the "water savings" effect, and disappears completely when leaf area is increased in eC_a, as was the case in the cherry experiment.

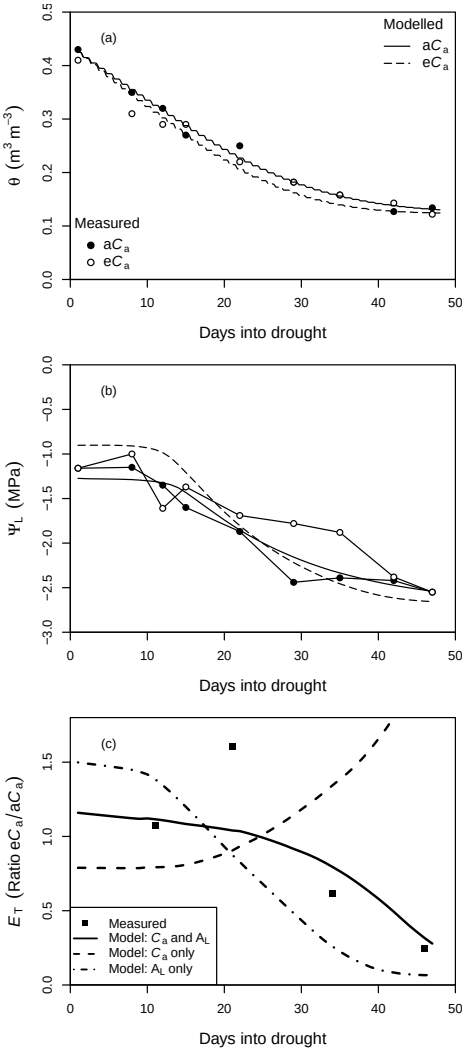

Fig. 6. Application of MAESPA to an experiment on droughted cherry seedlings by Centritto et al. (1999a, b). Model parameters were based on reported values in the original study, or calibrated to yield a satisfactory fit to the data of the aC_a treatment only (see text and Table 2). The optimized parameter set was then used to predict water balance in the eC_a treatment, and taking into account the observed increase in leaf area in the eC_a seedlings. **(a)** Decline in average soil water content over the rooting zone (θ) as the drought progressed. **(b)** Decline in the midday leaf water potential for sunlit foliage (Ψ_L). Note a relatively poor fit for the eC_a treatment: Ψ_L is over-predicted early in the drought, and under-predicted towards the end of the drought. **(c)** The ratio of total water use in eC_a to aC_a during the dry-down. Higher leaf area in eC_a initially leads to higher water use, but this leads to lower θ **(a)** and Ψ_L **(b)**, so that eC_a seedlings were more water-stressed toward the end of the dry-down than their aC_a counterparts. The solid line shows the simulations where eC_a and the increase in leaf area in the eC_a treatment were taken into account, dashed lines show either the direct C_a effect only (without leaf area feedback) or the leaf area feedback only (no eC_a treatment).

4 Discussion

We have presented a new soil-plant-atmosphere model, MAESPA, that can be applied to both individual plant and whole stand scales. The model includes detailed radiation transfer and leaf physiology routines from the MAESTRA model, and mechanistic water balance and hydraulics from

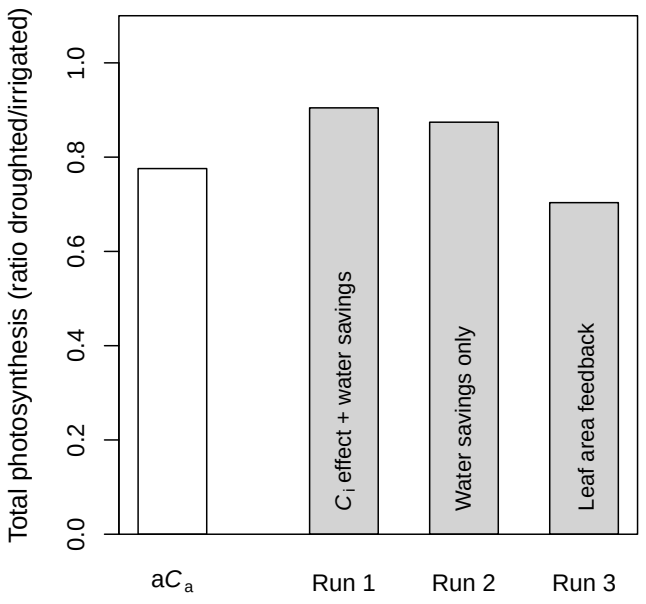

Fig. 7. Effect of the drought treatment on simulated total photosynthesis (summed over the entire 47 day simulation) for the dry-down in the cherry experiment (Fig. 6). The aC_a simulation shows a 22 % reduction in A_T in the dry-down treatment. For eC_a, three simulations are shown. Run 1: full simulation but without the leaf area feedback, Run 2: simulation at aC_a, but with reduced leaf area to match total water use in the eC_a simulation (Run 1), Run 3: including the observed leaf area increase in the eC_a treatment.

the SPA model. We have shown that the model gives realistic predictions of the response of several plant variables to drought. As an example application, we used the model to study the interaction between atmospheric [CO_2] (C_a) and drought.

4.1 Understanding controls on the C_a × drought interaction

In this paper, we illustrated the use of the MAESPA model by quantifying interactions between C_a and drought under several potential experimental scenarios. First we simulated our "baseline" expectation of the C_a × drought interaction, in the absence of feedbacks or acclimation of plant properties to long-term growth at eC_a. Experimental outcomes can be compared to simulations like these, in order to evaluate whether the results are in quantitatively in line with current understanding of biophysical and physiological controls on whole-plant gas exchange and water balance.

The MAESPA model was able to simulate the effects of a soil dry-down on several variables in line with published observations. During the dry-down, C_i/C_a steadily decreased, so that A_T/E_T increased, which is consistent with published studies where non-stomatal limitations to carbon uptake are minimal (Brodribb, 1996). Midday leaf water potential (Ψ_L) decreased steadily, as typically observed (Sperry, 2000), and leaf temperature increased as a result of lower stomatal conductance in dry soil (Jones, 1992; Triggs et al., 2004). Finally, the depth of root water uptake gradually shifted to deeper layers (cf. Rambal, 1984; Duursma et al., 2011).

The baseline simulations predict that total CO_2 uptake (A_T) is enhanced more by eC_a in dry soil (Fig. 5a), which is in line with previous predictions (Grossman-Clarke et al., 2001), and follows directly from the nonlinearity of the dependence of A_n on C_i (the "C_i effect"). The magnitude of this drought-enhanced eC_a response depends on the parameters used (in particular V_{cmax}, g_1), as well as the soil water content (Fig. 5a). Although many studies on agricultural crops have demonstrated that biomass growth or net canopy carbon uptake is more enhanced by eC_a during drought (Rogers et al., 1994), a great number of studies, particularly on trees, fail to demonstrate this effect (see Wullschleger et al., 2002; Nowak et al., 2004; Duursma et al., 2011; Warren et al., 2011). It should be noted that the interpretation of biomass growth in drought conditions is not straightforward because biomass growth may be temporally uncoupled from photosynthetic CO_2 uptake (Körner, 2003; Sala and Hoch, 2009). However, this is unlikely an explanation for the lack of observations for expected C_a × drought interaction in trees, because many studies report CO_2 uptake as well as biomass growth. We showed here that two plant parameters, that are frequently observed to be affected by acclimation to eC_a, can reduce or even reverse this expected interaction (Fig. 6). Some studies have found this "reverse" response: Schäfer et al. (2002) found that, in a FACE study on *Pinus taeda* L., E_L was only reduced by eC_a when soil was dry, which counters the baseline expectation of C_a responses (Fig. 6). In a FACE study on *Liquidambar styraciflua* L., Gunderson et al. (2002) found a higher sensitivity of g_s to Ψ_S in eC_a trees, which also has the potential to reverse the expected interaction between C_a and drought. We need to quantify the effect of such leaf acclimation to eC_a and investigate the degree to which it can explain experimental outcomes that diverge from baseline predictions. A model such as MAESPA is an essential tool to quantify the contribution of such mechanisms.

Baseline expectations are that lower leaf-level water use in eC_a will lead to a higher soil water content, thus delaying the onset of drought (Morgan et al., 2004). A drought treatment should therefore have less impact on total carbon uptake in eC_a than in an aC_a treatment, because drought stress is postponed (the "water savings" effect). However, testing this hypothesis against data from C_a × drought experiments can be difficult because increased plant size in eC_a often compensates for lower leaf-level water use, so that a clear "water savings" effect is often not directly observed (Morison and Gifford, 1984; Roden and Ball, 1996; Centritto et al., 1999a). We applied MAESPA to an experiment in cherry, where increased leaf area fully compensated for lower leaf-level water use. In this experiment, soil water content declined at similar rates in aC_a and eC_a treatments (Fig. 6), despite lower water use at the leaf-level in in eC_a, because leaf area was

ca. 50 % higher in the eC_a plants. The MAESPA model successfully simulated the compensation of total plant water use by increased leaf area, using one parameter set for both C_a treatments, and the measured leaf areas. Because of the leaf area feedback, Centritto et al. (1999a) concluded that there was no positive interaction between drought and C_a, a conclusion that followed from a standard empirical analysis of the results. Experiments like this can be further analysed in a quantitative framework like MAESPA, because plant leaf area can be quantitatively accounted for in the simulations, which is much more difficult to accomplish in a purely empirical analysis. Using the parameterized model, it is then possible to separate the various contributing factors to the overall $C_a \times$ drought interaction, and to estimate the strength of the interaction between C_a and drought.

Using the parameterized MAESPA model, we showed that there were interactions between C_a and drought in the cherry experiment. As the drought progressed, total plant water use declined more rapidly in the eC_a treatment (Fig. 6c), an experimental observation that was roughly matched by the model simulation (Fig. 6c). However, a poor fit to Ψ_L (Fig. 6b) was necessary to match the larger reduction in E_T in eC_a as the dry-down progressed (Fig. 6c). This mismatch is possibly because Ψ_L was sampled on a few sunlit leaves that were not representative of the entire canopy. Without the leaf area feedback, there was a strong simulated positive interaction of C_a and drought (Fig. 6c): water use could continue much longer in the eC_a treatment due to initial water savings. This analysis was therefore able to separate effects of leaf area and leaf-level processes on the response of plant water use to drought and C_a.

The interaction between C_a and drought is expected to particularly affect plant CO_2 uptake (A_T), because of the "C_i effect": photosynthesis is more responsive to C_a at low stomatal conductance, as is the case during drought (Fig. 5a). But what is the expected strength of this interaction, and is it more important than the "water savings" effect? For the cherry experiment, we calculated total A_T over the entire drying cycle, and expressed it as a ratio of droughted to irrigated control (Fig. 7). Drought reduced total A_T by a smaller fraction in the eC_a treatment compared to the aC_a treatment (10 % vs. 23 %). This relatively small difference is perhaps one reason that the $C_a \times$ drought interaction in experiments is often not significant, because there may be insufficient power to detect effects of this size. The simulation analysis demonstrated that the positive interaction was mostly a water savings effect in this case, the "C_i effect" was very small (Fig. 7). It is possible that the C_i effect is larger in other experiments, because it depends on the shape of the A–C_i curve, the degree of drought stress, stomatal conductance, and the length of the drought period.

Large scale simulations of C_a effects on vegetation water use and carbon uptake do not account for acclimation or feedbacks of plant processes to long-term growth at C_a (e.g. Cramer et al., 2001; Luo et al., 2008), and as such yield predictions of a positive $C_a \times$ drought interaction in line with the baseline predictions shown here (Fig. 4). However, actual experimental outcomes yield varied results, making it difficult to inform model formulation and parameterization with experimental data. Here, we showed that by taking into account the observed feedback of plant leaf area in one experiment, it is possible to study the C_a effect on plant water use and carbon uptake, had the feedback not occurred. A model like MAESPA can also be used to evaluate alternative explanations for the deviation from experimental outcomes from the expected theory, such as acclimation of plant hydraulic parameters (e.g. k_P, Ψ_f), and to evaluate whether responses at the leaf level match the responses at the whole-canopy scale.

4.2 Possible applications of MAESPA

While this study focussed on the interaction between C_a and drought, there are a number of possible applications of a soil-plant-atmosphere model that can be applied to whole-plant and forest stand scales. Analysis of complex experiments where data are collected at leaf-level, whole-tree or canopy level, and in the soil, can be strengthened if all data are integrated in the parameterization of a soil-plant-atmosphere model (Williams et al., 2001b; Medlyn et al., 2005; Duursma et al., 2007, 2009). Because MAESPA can be applied to potted plants, it may be used to generalize experimental results from the vast number of experiments on potted plants, that are typically confounded by changes in plant size with experimental treatments (e.g. Damesin et al., 1996).

There is a growing interest in the effects of stand structure on ecosystem functioning, because the spatial distribution of leaf area index (LAI) in sparse or dense crowns affects radiation interception, energy balance, and total water use (Chen et al., 2008; Yang et al., 2010), even though LAI is the primary driver for fluxes of water and carbon. The MAESPA model is well suited to study effects of canopy structure and grouping of foliage in tree crowns on whole-canopy performance, and to evaluate simplified approaches.

All currently available soil-plant-atmosphere models can only be applied to entire canopies, restricting their use to studying stand-level processes. The advantage of MAESPA is that single plants can be studied. For example, models of vegetation water use are typically tested against scaled-up sap-flux measurements (Hanson et al., 2004; Williams et al., 2001a; Zeppel et al., 2008). An individual-based model such as MAESPA can be used to address questions of resource distribution among plants of different size and species within a canopy (cf. Binkley et al., 2010), in particular regarding the use of soil water and response to soil drought.

4.3 Uncertainty in process representation

The quantitative understanding of a number of processes in the soil-plant-atmosphere continuum is limited, so that

improvements to models like MAESPA are certainly possible. Below, we discuss uncertainty in three components of MAESPA, but they apply to any soil-plant-atmosphere model: root water uptake, variation in plant hydraulic conductance, and non-stomatal limitations to CO_2 uptake during drought. These three components are just examples where progress in process understanding will improve soil-plant-atmosphere models; there are certainly others.

Predicting the distribution of root water uptake with depth in the soil is an old problem (Gardner, 1964), and surprisingly little progress has been made since the simple model advanced by Taylor and Keppler (1975), which is used in nearly all root water uptake models (Feddes et al., 2001). Although this approach seems relatively successful in predicting relative uptake of water from different soil layers (Markewitz et al., 2010), it is not useful in predicting the reduction in total water uptake when only a part of the root system is accessing wet soil, as is the case for chronically droughted trees that have few roots at great depth (Calder et al., 1997). A better understanding of the root hydraulic conductance and how it varies with depth in the soil, and the partitioning of the resistance between radial and longitudinal components of the root pathway are needed to improve on this model component.

It is typically assumed, as in MAESPA, that the decline in CO_2 uptake during drought is the result only of reduced stomatal conductance, which simply limits the diffusion of CO_2 into leaves. However, there is ample evidence that photosynthetic capacity (A_n at a given C_i) also declines during drought, albeit highly dependent on species and possibly only during more severe water stress (Lawlor and Cornic, 2002). Recently, Keenan et al. (2009) and Grant and Flanagan (2007) both showed that accounting for the reduction in photosynthetic capacity with drought stress improved model predictions of canopy fluxes. A more general understanding of non-stomatal limitations and how they develop during drought stress will improve models such as MAESPA.

In MAESPA, the hydraulic conductance of the plant pathway (k_P) does not decline during drought, and does not vary among shaded or sunlit portions of the canopy. Although k_P typically does decrease during drought due to formation of air-filled vessels (Sperry ,2000), Duursma et al. (2008) showed that a model assuming a fixed k_P was successful in predicting the response of plant water use to water limitation, in part because the soil resistance becomes limiting to water transport (Fisher et al., 2006). Nonetheless, gradual reduction in k_P during drought is often an important determinant of plant water use (Sperry et al., 1998; Hacke et al., 2000).

Differences in k_P between shaded and sunlit leaves in the canopy may exist because of shorter path length to shaded leaves, which increases k_P in shaded leaves relative to sunlit leaves (as assumed in the SPA model, Williams et al. ,1996), or more conductive tissues connecting sunlit leaves to the roots, which increases k_P in sunlit leaves (Lemoine et al., 2002). It is advantageous for plants to increase k_P to more productive parts of the crown (Katul et al., 2003), but it is as yet unclear how k_P actually varies within crowns. Recently, Peltoniemi et al. (2012) argued that it is optimal for plants to distribute total hydraulic conductance in a way that k_P is proportional to average PAR for any leaf in the canopy. If this hypothesis is confirmed with measurements, it greatly simplifies a difficult problem, and it can be readily implemented in MAESPA.

4.4 Conclusions

We have implemented a new tool to study single-plant or canopy-scale interactions between environmental drivers, canopy structure, weather, and soil water balance. The usefulness of a single-tree model has already been demonstrated by the broad user-base of the MAESTRA model. Here, we have widened the applicability by introducing detailed water balance components, and hydraulic constraints on water use and CO_2 uptake. The new model incorporates a finer level of mechanistic detail than simplified water balance models (e.g. Granier et al., 1999), while still being relatively straightforward to parameterize (see Table B1 for a list of required parameters for the water balance component).

We suggest a way forward in integrating diverse experimental results, by evaluating experimental outcomes in a quantitative framework that summarizes our understanding of the soil-plant-atmosphere continuum. We showed that even relatively straightforward interactions like the $C_a \times$ drought interaction can be highly variable, because they are dependent on feedbacks of plant size on the soil water balance and acclimation of plant properties due to long-term growth at C_a. Quantitative evaluation of the role of such feedbacks is essential if we are to advance our understanding of plant responses to environmental change. Too often in the current literature on C_a experiments, responses are simply presented as significant/not significant, rather than being compared quantitatively to expectations based on current theory. As argued by Phillips and Milo (2009), we need to move from asking "Was there a change?" to asking "How large was the change, and is that what we expected?"

Appendix A

List of symbols, their definition and units.

Table A1. List of symbols, their definition and units.

Model inputs and constants	
J_{max}	Maximum rate of electron transport ($\mu mol\ m^{-2}\ s^{-1}$)
V_{cmax}	Maximum rate of Rubisco activity ($\mu mol\ m^{-2}\ s^{-1}$)
I_R	Fraction inhibition of R_d in the light (–)
C_a	Atmospheric CO_2 concentration ($\mu mol\ mol^{-1}$)
γ	Shape parameter of the light response of electron transport (–)
$g_0 g_s$	when A_n is zero (residual stomatal conductance) ($mol\ m^{-2}\ s^{-1}$)
g_1	Slope parameter of a Ball-Berry-type model of g_s (units depend on units of $f(D)$)
Ψ_{min}	Minimum leaf water potential (Ball-Berry model) (MPa)
Ψ_f	Ψ_L where $f_{\Psi L} = 0.5$ (Tuzet model) (MPa)
s_f	Steepness of the $f_{\Psi L}$ function (Tuzet model) (–)
k_P	Plant component of the leaf-specific hydraulic conductance ($mmol\ m^{-2}\ s^{-1}\ MPa^{-1}$)
u_z	Above-canopy wind speed ($m\ s^{-1}$)
z_H	Measurement height of wind speed (m)
z_0	Roughness length (m)
z_D	Zero plane displacement (m)
ϕ	Infiltration parameter (–)
z_i	Soil depth to the bottom of layer i (m)
Z	Total soil depth (m)
β	Root distribution parameter (–)
Ψ_{Rmin}	Minimum root water potential (no uptake below this value) (MPa)
ω_s	Tortuosity of the soil air space (–)
$L_{d,min}$	Minimum thickness of the dry soil surface layer (m)
L_v	Fine root density (varies by soil layer) ($m\ m^{-3}$)
r_1	Fraction throughfall of rain through canopy (–)
r_2,r_3	Canopy drainage parameters (mm and –)
θ_{sat}	Soil porosity (water content at saturation) (varies by layer) ($m^3\ m^{-3}$)
K_{sat}	Saturated soil hydraulic conductivity (varies by layer) ($mol\ m^{-1}\ s^{-1}\ MPa^{-1}$)
Ψ_e	Parameter for the soil water retention curve (MPa)
b	Parameter for the soil water retention curve (–)
r_r	Mean fine root radius (m)
L_T	Canopy leaf area index ($m^2\ m^{-2}$)
T_{air}	Air temperature (°C)
Model variables, constants, and outputs	
A_c	Rubisco-activity limited gross leaf photosynthesis rate ($\mu mol\ m^{-2}\ s^{-1}$)
A_j	RuBP-regeneration limited gross leaf photosynthesis rate ($\mu mol\ m^{-2}\ s^{-1}$)
A_n	Net photosynthetic CO_2 uptake rate ($\mu mol\ m^{-2}\ s^{-1}$)
A_T	Total canopy CO_2 uptake rate ($\mu mol\ m^{-2}$ (ground) s^{-1})
R_d	Dark respiration ($\mu mol\ m^{-2}\ s^{-1}$)
C_i	Intercellular CO_2 concentration ($\mu mol\ mol^{-1}$)
C_s	CO_2 concentration at the leaf surface ($\mu mol\ mol^{-1}$)
Q	Photosynthetic photon flux density at the leaf level ($\mu mol\ m^{-2}\ s^{-1}$)
J	Electron transport rate ($\mu mol\ m^{-2}\ s^{-1}$)
Γ^*	CO_2-compensation point in the absence of dark respiration ($\mu mol\ mol^{-1}$)
g_s, g_C	Stomatal conductance to H_2O (g_s) and CO_2 (g_c) ($mol\ m^{-2}\ s^{-1}$)
Ψ_L	Bulk leaf water potential (MPa)
$\Psi_{S,i}$	Soil water potential in soil layer i (MPa)
Ψ_R	Mean root xylem water potential (MPa)
D	Leaf-to-air vapour pressure deficit (kPa)
k_L	Leaf-specific hydraulic conductance ($mmol\ m^{-2}\ s^{-1}\ MPa^{-1}$)
λ	Latent heat of water vapour ($J\ mol^{-1}$)
s	The slope of the relation between saturation vapour pressure and temperature ($Pa\ K^{-1}$)
R_n	Net radiation ($W\ m^{-2}$)
g_B	Boundary layer conductance ($mol\ m^{-2}\ s^{-1}$)
g_V	Total conductance to water vapour ($mol\ m^{-2}\ s^{-1}$)
s_i	Soil water storage in layer i (mm)
I_i	Infiltration into layer i (mm)
D_i	Drainage out of layer i (mm)
E_i	Root water uptake (canopy transpiration) out of layer i (mm)
E_s	Soil surface evaporation (mm)
E_w	Canopy wet evaporation rate ($mm\ timestep^{-1}$)

Table A1. Continued.

E_L	Leaf-level transpiration rate (mmol m^{-2} s^{-1})
E_T	Canopy transpiration (for use in water balance) (mol m^{-2} (ground) s^{-1})
R_{sr}	Soil-to-root surface hydraulic resistance (MPa s m^2 mol^{-1})
$G_{s,t}$	Total conductance to water vapour from soil air space to air above the soil boundary layer (m s^{-1})
e_s	Partial water vapour pressure of the soil pore space (kPa)
e_a	Partial water vapour pressure of the air above the soilk boundary layer (kPa)
G_{ws}	Conductance of water vapour through the soil pore space (m s^{-1})
D_{eff}	Effective diffusivity of the soil pore space (m^2 s^{-1})
L_d	Thickness of the dry layer at the soil surface (m)
D_w	Diffusivity of water vapour (function of soil temperature) (m^2 s^{-1})
k_V	von Karman's constant (= 0.41) (–)
T_i	Soil temperature of layer i (°C)
W_{can}	Water storage of the canopy (mm)
θ_i	Soil volumetric water content of layer i (m^3 m^{-3})
K_s	Soil hydraulic conductivity (mol m^{-1} s^{-1} MPa^{-1})
r_s	Mean distance between roots (m)
Q_n	Soil surface net radiation (W m^{-2})
Q_e	Soil latent heat flux (W m^{-2})
Q_h	Soil sensible heat flux (W m^{-2})
Q_c	Soil heat transport (W m^{-2})
K_{th}	Soil thermal conductivity (W m^{-1} K^{-1})
ε	Soil surface emissivity (–)
σ	Stefan-Boltzmann constant (W m^{-2} K^{-4})
c_p	Heat capacity of air (constant) (J kg^{-1} K^{-1})
ρ	Density of air (kg m^{-3})
$G_{a,m}$	The boundary layer conductance to heat transfer (mol m^{-2} s^{-1})

Appendix B

Below we have summarized the list of parameters needed to simulate the various components of the soil water balance and the response of plant water use to soil water deficit. Parameters that have very little influence or are likely to be near constant are not listed, nor are variables that are derived from the inputs and other constants. An example is fine root density, which has little influence on water uptake apart from the relative distribution of roots in different layers.

Table B1. List of parameters needed to simulate the water balance.

k_P	Plant component of the leaf-specific hydraulic conductance (mmol m^{-2} s^{-1} MPa^{-1})
Ψ_{min}	Minimum leaf water potential (only when using Ball-Berry model) (MPa)
Ψ_f	Ψ_L where $f_{\Psi L} = 0.5$ (only when using Tuzet model) (MPa)
s_f	Steepness of the $f_{\Psi L}$ function (only when using Tuzet model) (–)
Z	Total soil depth (m)
β	Root distribution parameter (–) (or layer-wise specification of rooting density)
r_1	Fraction throughfall of rain through canopy (–)
r_2, r_3	Canopy drainage parameters (mm and –)
θ_{sat}	Soil porosity (water content at saturation) (varies by layer) (m^3 m^{-3})
K_{sat}	Saturated soil hydraulic conductivity (varies by layer) (mol m^{-1} s^{-1} MPa^{-1})
Ψ_e	Parameter for the soil water retention curve (MPa)
b	Parameter for the soil water retention curve (–)
ω_s	Tortuosity of the soil air space (–) (only needed for soil evaporation)
$L_{d,min}$	Minimum thickness of the dry soil surface layer (m) (only needed for soil evaporation)

Acknowledgements. We thank Mat Williams for providing the source code of the SPA model and encouraging a fusion with the MAESTRA model. RAD was supported by NSW Government Climate Action Grant (NSW T07/CAG/016). We thank Rhys Whitley for discussing SPA and Fortran, and Martin de Kauwe for additional coding and bug chasing.

Edited by: D. Lawrence

References

Ainsworth, E. A. and Long, S. P.: What have we learned from 15 years of free-air CO_2 enrichment (FACE)? A meta-analytic review of the responses of photosynthesis, canopy properties and plant production to rising CO_2, New Phytol., 165, 351–371, 2005.

Ainsworth, E. A. and Rogers, A.: The response of photosynthesis and stomatal conductance to rising [CO_2]: mechanisms and environmental interactions, Plant Cell Environ., 30, 258–270, doi:10.1111/j.1365-3040.2007.01641.x, 2007.

Atkinson, C. and Taylor, J.: Effects of elevated CO_2 on stem growth, vessel area and hydraulic conductivity of oak and cherry seedlings, New Phytol., 133, 617–626, 1996.

Ball, J. T., Woodrow, I. E., and Berry, J. A.: A model predicting stomatal conductance and its contribution to the control of photosynthesis under different environmental conditions., in: Progress in photosynthesis research, edited by: Biggins, J., Martinus-Nijhoff Publishers, Dordrecht, the Netherlands, 221–224, 1987.

Barton, C. V. M., Ellsworth, D. S., Medlyn, B. E., Duursma, R. A., Tissue, D. T., Adams, M. A., Eamus, D., Conroy, J. P., McMurtrie, R. E., Parsby, J., and Linder, S.: Whole-tree chambers for elevated atmospheric CO_2 experimentation and tree scale flux measurements in south-eastern Australia: The Hawkesbury Forest Experiment, Agr. Forest Meteorol., 150, 941–951, 2010.

Bauerle, W. L. and Bowden, J. D.: Separating foliar physiology from morphology reveals the relative roles of vertically structured transpiration factors within red maple crowns and limitations of larger scale models, J. Exp. Bot., 62, 4295–4307, 2011.

Berryman, C. A., Eamus, D., and Duff, G. A.: Stomatal responses to a range of variables in two tropical tree species grown with CO_2 enrichment, J. Exp. Bot., 45, 539–546, doi:10.1093/jxb/45.5.539, 1994.

Binkley, D., Stape, J. L., Bauerle, W. L., and Ryan, M. G.: Explaining growth of individual trees: Light interception and efficiency of light use by Eucalyptus at four sites in Brazil, For. Ecol. Manage., 259, 1704–1713, 2010.

Bristow, K. L. and Campbell, G. S.: On the relationship between incoming solar radiation and daily maximum and minimum temperature, Agr. Forest Meteorol., 31, 159–166, 1984.

Brodribb, T.: Dynamics of changing intercellular CO_2 concentration (ci) during drought and determination of minimum functional ci, Plant Physiol., 111, 179–185, 1996.

Calder, I. R., Rosier, P. T. W., Prasanna, K. T., and Parameswarappa, S.: Eucalyptus water use greater than rainfall input – possible explanation from southern India, Hydrol. Earth Syst. Sci., 1, 249–256, doi:10.5194/hess-1-249-1997, 1997.

Campbell, G. S.: A simple method for determining unsaturated conductivity from moisture retention data, Soil Sci., 117, 311–314, 1974.

Centritto, M., Lee, H. S. J., and Jarvis, P. G.: Interactive effects of elevated [CO_2] and drought on cherry (*Prunus avium*) seedlings, I. Growth, whole-plant water use efficiency and water loss, New Phytol., 141, 129–140, 1999a.

Centritto, M., Magnani, F., Lee, H. S. J., and Jarvis, P. G.: Interactive effects of elevated [CO_2] and drought on cherry (*Prunus avium*) seedlings, II. Photosynthetic capacity and water relations, New Phytol., 141, 141–153, 1999b.

Chen, Q., Baldocchi, D., Gong, P., and Dawson, T.: Modeling radiation and photosynthesis of a heterogeneous savanna woodland landscape with a hierarchy of model complexities, Agr. Forest Meteorol., 148, 1005–1020, 2008.

Choudhury, B. J. and Monteith, J. L.: A four-layer model for the heat budget of homogeneous land surfaces, Q. J. Roy. Meteorol. Soc., 114, 373–398, 1988.

Comstock, J. and Mencuccini, M.: Control of stomatal conductance by leaf water potential in *Hymenoclea salsola* (T. & G.), a desert subshrub, Plant, Cell Environ., 21, 1029–1038, doi:10.1046/j.1365-3040.1998.00353.x, 1998.

Cosby, B. J., Hornberger, G. M., Clapp, R. B., and Ginn, T. R.: A statistical exploration of the relationships of soil-moisture characteristics to the physical properties of soils, Water Resour. Res., 20, 682–690, 1984.

Cowan, I. and Farquhar, G. D.: Stomatal function in relation to leaf metabolism and environment, Sym. Soc. Exp. Biol., 31, 471–505, 1977.

Cramer, W., Bondeau, A., Woodward, F. I., Prentice, I. C., Betts, R. A., Brovkin, V., Cox, P. M., Fisher, V., Foley, J. A., and Friend, A. D.: Global response of terrestrial ecosystem structure and function to CO_2 and climate change: results from six dynamic global vegetation models, Glob. Change Biol., 7, 357–373, 2001.

Damesin, C., Galera, C., Rambal, S., and Joffre, R.: Effects of elevated carbon dioxide on leaf gas exchange and growth of cork-oak (Quercus suber L) seedlings, Ann. Sci. For., 53, 461–467, 1996.

de Vries, D. A.: Thermal properties of soils, in: Physics of plant environment, edited by: van Wijk, W. R., Amsterdam, 210–235, 1963.

Delzon, S., Sartore, M., Burlett, R., Dewar, R. C., and Loustau, D.: Hydraulic responses to height growth in maritime pine trees., Plant, Cell Environ., 27, 1077–1087, 2004.

Domec, J.-C., Ogée, J., Noormets, A., Jouangy, J., Gavazzi, M., Treasure, E., Sun, G., McNulty, S. G., and King, J. S.: Interactive effects of nocturnal transpiration and climate change on the root hydraulic redistribution and carbon and water budgets of southern United States pine plantations, Tree Physiol., 32, 707–723, doi:10.1093/treephys/tps018, 2012.

Dubbe, D. R., Farquhar, G. D., and Raschke, K.: Effect of abscisic acid on the gain of the feedback loop involving carbon dioxide and stomata, Plant Physiol., 62, 413–417, 1978.

Duursma, R. A., Marshall, J. D., Robinson, A. P., and Pangle, R. E.: Description and test of a simple process-based model of forest growth for mixed-species stands, Ecol. Model., 203, 297–311, 2007.

Duursma, R. A., Kolari, P., Perämäki, M., Nikinmaa, E., Hari, P., Delzon, S., Loustau, D., Ilvesniemi, H., Pumpanen, J., and Mäkelä, A.: Predicting the decline in daily maximum transpiration rate of two pine stands during drought based on constant minimum leaf water potential and plant hydraulic conductance,

Tree Physiol., 28, 265–276, 2008.

Duursma, R. A., Kolari, P., Perämäki, M., Pulkkinen, M., Mäkelä, A., Nikinmaa, E., Hari, P., Aurela, M., Berbigier, P., Bernhofer, C., Grünwald, T., Loustau, D., Mölder, M., Verbeeck, H., and Vesala, T.: Contributions of climate, leaf area index and leaf physiology to variation in gross primary production of six coniferous forests across Europe: a model-based analysis, Tree Physiol., 29, 621–639, 2009.

Duursma, R. A., Barton, C. V. M., Eamus, D., Medlyn, B. E., Ellsworth, D. S., Forster, M. A., Tissue, D. T., Linder, S., and McMurtrie, R. E.: Rooting depth explains [CO_2]?×?drought interaction in *Eucalyptus saligna*, Tree Physiol., 31, 922–931, doi:10.1093/treephys/tpr030, 2011.

Eamus, D.: The interaction of rising CO_2 and temperatures with water use efficiency, Plant, Cell Environ., 14, 843–852, 1991.

Eamus, D., Berryman, C., and Duff, G.: The Impact of CO_2 Enrichment on Water Relations in *Maranthes corymbosa* and *Eucalyptus tetrodonta*, Aust. J. Bot., 43, 273–282, doi:10.1071/BT9950273, 1995.

Eguchi, N., Morii, N., Ueda, T., Funada, R., Takagi, K., Hiura, T., Sasa, K., and Koike, T.: Changes in petiole hydraulic properties and leaf water flow in birch and oak saplings in a CO_2-enriched atmosphere, Tree Physiol., 28, 287–295, doi:10.1093/treephys/28.2.287, 2008.

Farquhar, G. D., Caemmerer, S., and Berry, J. A.: A biochemical model of photosynthetic CO_2 assimilation in leaves of C3 species, Planta, 149, 78–90, 1980.

Feddes, R. A., Hoff, H., Bruen, M., Dawson, T., de Rosnay, P., Dirmeyer, O., Jackson, R. B., Kabat, P., Kleidon, A., Lilly, A., and Pitman, A. J.: Modeling root water uptake in hydrological and climate models, Bull. Am. Meteorol. Soc., 82, 2797–2809, 2001.

Federer, C., Vörösmarty, C., and Fekete, B.: Sensitivity of annual evaporation to soil and root properties in two models of contrasting complexity, J. Hydrometeorol., 4, 1276–1290, 2003.

Fisher, R. A., Williams, M., Do Vale, R. L., Da Costa, A. L., and Meir, P.: Evidence from Amazonian forests is consistent with isohydric control of leaf water potential, Plant Cell Environ., 29, 151–165, 2006.

Franks, P. J.: Stomatal control and hydraulic conductance, with special reference to tall trees, Tree Physiol., 24, 865–878, 2004.

Gardner, W. R.: Dynamic aspects of water availability to plants, Soil Sci., 89, 63–73, 1960.

Gardner, W. R.: Relation of Root Distribution to Water Uptake and Availability, Agron. J., 56, 41–45, 1964.

Granier, A., Breda, N., Biron, P., and Villette, S.: A lumped water balance model to evaluate duration and intensity of drought constraints in forest stands, Ecol. Model., 116, 269–283, 1999.

Grant, R. F. and Flanagan, L. B.: Modeling stomatal and nonstomatal effects of water deficits on CO2 fixation in a semiarid grassland, J. Geophys. Res., 112, G03011, doi:10.1029/2006jg000302, 2007.

Grossman-Clarke, S., Pinter Jr., P., Kartschall, T., Kimball, B., Hunsaker, D., Wall, G., Garcia, R., and LaMorte, R.: Modelling a spring wheat crop under elevated CO_2 and drought, New Phytol., 150, 315–335, 2001.

Gunderson, C. A., Sholtis, J. D., Wullschleger, S. D., Tissue, D. T., Hanson, P. J., and Norby, R. J.: Environmental and stomatal control of photosynthetic enhancement in the canopy of a sweetgum (*Liquidambar styraciflua* L.) plantation during 3 years of CO_2 enrichment, Plant Cell Environ., 25, 379–393, 2002.

Hacke, U. G., Sperry, J. S., Ewers, B. E., Ellsworth, D. S., Schafer, K. V. R., and Oren, R.: Influence of soil porosity on water use in Pinus taeda, Oecologia, 124, 495–505, 2000.

Hanson, P. J., Amthor, J. S., Wullschleger, S. D., Wilson, K. B., Grant, R. F., Hartley, A., Hui, D., Hunt, E. R., Johnson, D. W., Kimball, J. S., King, A. W., Luo, Y., McNulty, S. G., Sun, G., Thornton, P. E., Wang, S., Williams, M., Baldocchi, D. D., and Cushman, R. M.: Oak forest carbon and water simulations: Model intercomparisons and evaluations against independent data, Ecol. Monogr., 74, 443–489, 2004.

Heath, J., Kerstiens, G., and Tyree, M.: Stem hydraulic conductance of European beech (*Fagus sylvatica* L.) and pedunculate oak (*Quercus robur* L.) grown in elevated CO_2, J. Exp. Bot., 48, 1487–1489, 1997.

Huntington, T. G.: Evidence for intensification of the global water cycle: Review and synthesis, J. Hydrol., 319, 83–95, 2006.

Jackson, R. B., Canadell, J., Ehleringer, J. R., Mooney, H. A., Sala, O. E., and Schulze, E. D.: A global analysis of root distributions for terrestrial biomes, Oecologia, 108, 389–411, 1996.

Jones, H. G.: Plants and microclimate: a quantitative approach to environmental plant physiology, 2nd Edn., Cambridge University Press, Cambridge, 428 pp., 1992.

Katul, G., Leuning, R., and Oren, R.: Relationship between plant hydraulic and biochemical properties derived from a steady-state coupled water and carbon transport model, Plant Cell Environ., 26, 339–350, 2003.

Keenan, T., García, R., Friend, A. D., Zaehle, S., Gracia, C., and Sabate, S.: Improved understanding of drought controls on seasonal variation in Mediterranean forest canopy CO2 and water fluxes through combined in situ measurements and ecosystem modelling, Biogeosciences, 6, 1423–1444, doi:10.5194/bg-6-1423-2009, 2009.

Kirschbaum, M., King, D., Comins, H., McMurtrie, R., Medlyn, B., Pongracic, S., Murty, D., Keith, H., Raison, R., and Khanna, P.: Modelling forest response to increasing CO_2 concentration under nutrient-limited conditions, Plant, Cell Environ., 17, 1081–1099, 1994.

Körner, C.: Carbon limitation in trees, J. Ecol., 91, 4–17, 2003.

Kruijt, B., Barton, C., Rey, A., and Jarvis, P. G.: The sensitivity of stand-scale photosynthesis and transpiration to changes in atmospheric CO_2 concentration and climate, Hydrol. Earth Syst. Sci., 3, 55–69, doi:10.5194/hess-3-55-1999, 1999.

Lawlor, D. and Cornic, G.: Photosynthetic carbon assimilation and associated metabolism in relation to water deficits in higher plants, Plant, Cell Environ., 25, 275–294, 2002.

Lemoine, D., Cochard, H., and Granier, A.: Within crown variation in hydraulic architecture in beech (Fagus sylvatica L): evidence for a stomatal control of xylem embolism, Ann. Forest Sci., 59, 19–27, 2002.

Leuning, R.: A Critical-Appraisal of a Combined Stomatal-Photosynthesis Model for C-3 Plants, Plant Cell Environ., 18, 339–355, 1995.

Lu, S., Ren, T., Gong, Y., and Horton, R.: An improved model for predicting soil thermal conductivity from water content at room temperature, Soil Sci. Soc. Am. J., 71, 8–14, doi:10.2136/sssaj2006.0041, 2007.

Luo, Y., Medlyn, B., Hui, D., Ellsworth, D., Reynolds, J., and Katul, G.: Gross primary productivity in duke forest: Modeling synthesis of CO_2 experiment and eddy-flux data, Ecol. Appl., 11, 239–252, 2001.

Luo, Y., Gerten, D., Le Maire, G., Parton, W. J., Weng, E., Zhou, X., Keough, C., Beier, C., Ciais, P., and Cramer, W.: Modeled interactive effects of precipitation, temperature, and $[CO_2]$ on ecosystem carbon and water dynamics in different climatic zones, Glob. Change Biol., 14, 1986–1999, 2008.

Luxmoore, R. J., Hargrove, W. W., Tharp, M. L., Post, W. M., Berry, M. W., Minser, K. S., Cropper, W. P., Johnson, D. W., Zeide, B., and Amateis, R. L.: Signal-transfer modeling for regional assessment of forest responses to environmental changes in the southeastern united states, Environ. Model. Assess., 5, 125–137, 2000.

Manzoni, S., Vico, G., Katul, G., Fay, P. A., Polley, W., Palmroth, S., and Porporato, A.: Optimizing stomatal conductance for maximum carbon gain under water stress: a meta-analysis across plant functional types and climates, Funct. Ecol., 25, 456–467, doi:10.1111/j.1365-2435.2010.01822.x, 2011.

Markewitz, D., Devine, S., Davidson, E. A., Brando, P., and Nepstad, D. C.: Soil moisture depletion under simulated drought in the Amazon: impacts on deep root uptake, New Phytol., 187, 592–607, 2010.

McAdam, S. A. M., Brodribb, T. J., Ross, J. J., and Jordan, G. J.: Augmentation of abscisic acid (ABA) levels by drought does not induce short-term stomatal sensitivity to CO_2 in two divergent conifer species, J. Exp. Bot., 62, 195–203, doi:10.1093/jxb/erq260, 2011.

McMurtrie, R. E., Norby, R. J., Medlyn, B. E., Dewar, R. C., Pepper, D. A., Reich, P. B., and Barton, C. V. M.: Why is plant-growth response to elevated CO_2 amplified when water is limiting, but reduced when nitrogen is limiting? A growth-optimisation hypothesis, Funct. Plant Biol., 35, 521–534, doi:10.1071/FP08128, 2008.

Medlyn, B. E.: Interactive effects of atmospheric carbon dioxide and leaf nitrogen concentration on canopy light use efficiency: a modeling analysis, Tree Physiol., 16, 201–209, 1996.

Medlyn, B. E.: A MAESTRO Retrospective, in: Forests at the Land-Atmosphere Interface, edited by: Mencuccini, M., Grace, J., Moncrieff, J. B., and McNaughton, K., CAB International, 105–121, 2004.

Medlyn, B. E., Barton, C. V. M., Broadmeadow, M. S. J., Ceulemans, R., De Angelis, P., Forstreuter, M., Freeman, M., Jackson, S. B., Kellomaki, S., Laitat, E., Rey, A., Roberntz, P., Sigurdsson, B. D., Strassemeyer, J., Wang, K., Curtis, P. S., and Jarvis, P. G.: Stomatal conductance of forest species after long-term exposure to elevated CO_2 concentration: a synthesis, New Phytol., 149, 247–264, 2001.

Medlyn, B. E., Dreyer, E., Ellsworth, D., Forstreuter, M., Harley, P. C., Kirschbaum, M. U. F., Le Roux, X., Montpied, P., Strassemeyer, J., Walcroft, A., Wang, K., and Loustau, D.: Temperature response of parameters of a biochemically based model of photosynthesis, II. A review of experimental data, Plant Cell Environ., 25, 1167–1179, 2002.

Medlyn, B. E., Berbigier, P., Clement, R., Grelle, A., Loustau, D., Linder, S., Wingate, L., Jarvis, P. G., Sigurdsson, B. D., and McMurtrie, R. E.: Carbon balance of coniferous forests growing in contrasting climates: Model-based analysis, Agr. Forest Meteorol., 131, 97–124, 2005.

Medlyn, B. E., Pepper, D. A., O'Grady, A. P., and Keith, H.: Linking leaf and tree water use with an individual-tree model, Tree Physiol., 27, 1687–1699, 2007.

Medlyn, B. E., Duursma, R. A., Eamus, D., Ellsworth, D. S., Prentice, I. C., Barton, C. V. M., Crous, K. Y., De Angelis, P., Freeman, M., and Wingate, L.: Reconciling the optimal and empirical approaches to modelling stomatal conductance, Glob. Change Biol., 17, 2134–2144, doi:10.1111/j.1365-2486.2010.02375.x, 2011.

Morgan, J., Pataki, D. E., Körner, C., Clark, H., del Grosso, S. J., Grunzweig, J. M., Knapp, A., Mosier, A. R., Newton, P. C. D., Niklaus, P. A., Nippert, J. B., Nowak, R. S., Parton, W. J., Polley, H. W., and Shaw, M. R.: Water relations in grassland and desert ecosystems exposed to elevated atmospheric CO_2, Oecologia, 140, 11–25, 2004.

Morison, J. and Gifford, R.: Plant growth and water use with limited water supply in high CO_2 concentrations, II. Plant dry weight, partitioning and water use efficiency, Funct. Plant Biol., 11, 375–384, doi:10.1071/PP9840375, 1984.

Mott, K. A.: Do stomata respond to CO_2 concentrations other then intercellular?, Plant Physiol., 86, 200–203, 1988.

Norby, R. and Luo, Y.: Evaluating ecosystem responses to rising atmospheric CO_2 and global warming in a multi-factor world, New Phytol., 162, 281–293, 2004.

Norby, R. J., Wullschleger, S. D., Gunderson, C. A., Johnson, D. W., and Ceulemans, R.: Tree responses to rising CO_2 in field experiments: implications for the future forest, Plant, Cell Environ., 22, 683–714, 1999.

Norman, J. M.: Modeling the complete crop canopy, in: Modification of the aerial environment of plants, edited by: Barfield, B. J., and Gerber, J. F., ASAE Monographs, American Soc. Agr. Eng., 2, 248–277, 1979.

Norman, J. M.: Scaling processes between leaf and canopy levels, in: Scaling physiological processes: leaf to globe, edited by: Ehleringer, J. R. and Field, C. B., Academic Press, San Diego, 41–76, 1993.

Norman, J. M. and Welles, J. M.: Radiative transfer in an array of canopies, Agron. J., 75, 481–488, 1983.

Nowak, R., Zitzer, S., Babcock, D., Smith-Longozo, V., Charlet, T., Coleman, J., Seemann, J., and Smith, S.: Elevated atmospheric CO_2 does not conserve soil water in the Mojave Desert, Ecology, 85, 93–99, 2004.

Ogée, J., Lamaud, E., Brunet, Y., Berbigier, P., and Bonnefond, J. M.: A long-term study of soil heat flux under a forest canopy, Agr. Forest Meteorol., 106, 173–186, 2001.

Peltoniemi, M., Duursma, R. A., and Medlyn, B. E.: Co-optimal distribution of leaf nitrogen and hydraulic conductance in plant canopies, Tree Physiol., 32, 510–519, doi:10.1093/treephys/tps023, 2012.

Phillips, R. and Milo, R.: A feeling for the numbers in biology, Proc. Nat. Aca. Sci., 106, 21465–21471, doi:10.1073/pnas.0907732106, 2009.

Pierce, M. and Raschke, K.: Synthesis and metabolism of abscisic acid in detached leaves of *Phaseolus vulgaris* L. after loss and recovery of turgor, Planta, 153, 156–165, 1981.

Poorter, H. and Navas, M.: Plant growth and competition at elevated CO_2: on winners, losers and functional groups, New Phytol., 157, 175–198, 2003.

Press, W. H., Teukolsky, S. L. A., Flannery, B. N. P., and Vetterling, W. M. T.: Numerical Recipes: FORTRAN, Cambridge university press, 1990.

R Development Core Team R: A language and environment for statistical computing. R Foundation for Statistical Computing, Vienna, Austria, ISBN 3-900051-07-0, available at: http://www.R-project.org/, 2011.

Rambal, S.: Water balance and pattern of root water uptake by a *Quercus coccifera* L. evergreen srub, Oecologia, 62, 18–25, 1984.

Reynolds, R. F., Bauerle, W. L., and Wang, Y.: Simulating carbon dioxide exchange rates of deciduous tree species: Evidence for a general pattern in biochemical changes and water stress response, Ann. Bot., 104, 775–784, doi:10.1093/aob/mcp156, 2009.

Roden, J. and Ball, M.: The effect of elevated [CO_2] on growth and photosynthesis of two eucalyptus species exposed to high temperatures and water deficits, Plant Physiol., 111, 909–919, 1996.

Rogers, H., Runion, G., and Krupa, S.: Plant responses to atmospheric CO_2, enrichment with emphasis on roots and the rhizosphere, Environ. Pollut., 83, 155–189, 1994.

Rustad, L. R., Campbell, J. C., Marion, G. M., Norby, R. N., Mitchell, M. M., Hartley, A. H., Cornelissen, J. C., Gurevitch, J. G., and Gcte-News, G.-N.: A meta-analysis of the response of soil respiration, net nitrogen mineralization, and aboveground plant growth to experimental ecosystem warming, Oecologia, 126, 543–562, doi:10.1007/s004420000544, 2001.

Rutter, A. J., Morton, A. J., and Robins, P. C.: A predictive model of rainfall interception in forests, III. Generalization of the model and comparison with observations in some coniferous and hardwood stands, J. Appl. Ecol., 12, 367–380, 1975.

Sala, A. and Hoch, G.: Height-related growth declines in ponderosa pine are not due to carbon limitation, Plant Cell Environ., 32, 22–30, 2009.

Saxton, K. E. and Rawls, W. J.: Soil water characteristic estimates by texture and organic matter for hydrologic solutions, Soil Sci. Soc. Am. J., 70, 1569–1578, doi:10.2136/sssaj2005.0117, 2006.

Schäfer, K. V. R., Oren, R., Lai, C. T., and Katul, G. G.: Hydrologic balance in an intact temperate forest ecosystem under ambient and elevated atmospheric CO_2 concentration, Glob. Change Biol., 8, 895–911, 2002.

Schaudt, K. J. and Dickinson, R. E.: An approach to deriving roughness length and zero-plane displacement height from satellite data, prototyped with BOREAS data, Agr. Forest Meteorol., 104, 143–155, 2000.

Schmidhalter, U.: The gradient between pre-dawn rhizoplane and bulk soil matric potentials, and its relation to the pre-dawn root and leaf water potentials of four species, Plant Cell Environ., 20, 953–960, 1997.

Sperry, J.: Hydraulic constraints on plant gas exchange, Agr. Forest Meteorol., 104, 13–23, 2000.

Sperry, J. S., Adler, F. R., Campbell, G. S., and Comstock, J. P.: Limitation of plant water use by rhizosphere and xylem conductance: results from a model, Plant Cell Environ., 21, 347–359, 1998.

Taylor, H. M. and Keppler, B.: Water uptake by cotton root systems: an examination of assumptions in the single root model, Soil Sci., 120, 57–67, 1975.

Triggs, J. M., Kimball, B. A., Pinter, P. J., Wall, G. W., Conley, M. M., Brooks, T. J., LaMorte, R. L., Adam, N. R., Ottman, M. J., Matthias, A. D., Leavitt, S. W., and Cerveny, R. S.: Free-air CO_2 enrichment effects on the energy balance and evapotranspiration of sorghum, Agr. Forest Meteorol., 124, 63–79, 2004.

Tuzet, A., Perrier, A., and Leuning, R.: A coupled model of stomatal conductance, photosynthesis and transpiration, Plant Cell Environ., 26, 1097–1116, 2003.

Wang, Y. P. and Jarvis, P. G.: Description and validation of an array model – MAESTRO, Agr. Forest Meteorol., 51, 257–280, 1990.

Wang, Y. P. and Leuning, R.: A two-leaf model for canopy conductance, photosynthesis and partitioning of available energy I: Model description and comparison with a multi-layered model, Agr. Forest Meteorol., 91, 89–111, 1998.

Wang, Y. P., Jarvis, P. G., and Benson, M. L.: Two-dimensional needle-area density distribution within the crowns of *Pinus radiata*, For. Ecol. Manage., 32, 217–237, 1990.

Warren, J. M., Pötzelsberger, E., Wullschleger, S. D., Thornton, P. E., Hasenauer, H., and Norby, R. J.: Ecohydrologic impact of reduced stomatal conductance in forests exposed to elevated CO_2, Ecohydrology, online first, doi:10.1002/eco.173, 2010.

Williams, M., Rastetter, E. B., Fernandes, D. N., Goulden, M. L., Wofsy, S. C., Shaver, G. R., Melillo, J. M., Munger, J. W., Fan, S. M., and Nadelhoffer, K. J.: Modelling the soil-plant-atmosphere continuum in a Quercus-Acer stand at Harvard forest: The regulation of stomatal conductance by light, nitrogen and soil/plant hydraulic properties, Plant Cell Environ., 19, 911–927, 1996.

Williams, M., Bond, B. J., and Ryan, M. G.: Evaluating different soil and plant hydraulic constraints on tree function using a model and sap flow data from ponderosa pine, Plant Cell Environ., 24, 679–690, 2001a.

Williams, M., Law, B. E., Anthoni, P. M., and Unsworth, M. H.: Use of a simulation model and ecosystem flux data to examine carbon-water interactions in ponderosa pine, Tree Physiol., 21, 287–298, 2001b.

Wu, Z., Dijkstra, P., Koch, G. W., Peñuelas, J., and Hungate, B. A.: Responses of terrestrial ecosystems to temperature and precipitation change: a meta-analysis of experimental manipulation, Glob. Change Biol., 17, 927–942, doi:10.1111/j.1365-2486.2010.02302.x, 2011.

Wullschleger, S. D., Tschaplinski, T. J., and Norby, R. J.: Plant water relations at elevated CO_2 – implications for water-limited environments, Plant, Cell Environ., 25, 319–331, 2002.

Yang, W., Ni-Meister, W., Kiang, N. Y., Moorcroft, P. R., Strahler, A. H., and Oliphant, A.: A clumped-foliage canopy radiative transfer model for a Global Dynamic Terrestrial Ecosystem Model II: Comparison to measurements, Agr. Forest Meteorol., 150, 895–907, 2010.

Zeppel, M., Macinnis-Ng, C., Palmer, A., Taylor, D., Whitley, R., Fuentes, S., Yunusa, I., Williams, M., and Eamus, D.: An analysis of the sensitivity of sap flux to soil and plant variables assessed for an Australian woodland using a soil-plant-atmosphere model, Funct. Plant Biol., 35, 509–520, doi:10.1071/FP08114, 2008.